

INVESTIGATION OF INDUCTIVE ENERGY
RELATIONSHIPS IN RELAY
MAGNETIC CIRCUITS .

BY

ROBERT AUSTIN CROMWELL

Bachelor of Science

Texas Agricultural and Mechanical College

College Station, Texas


August, 1950

Submitted to the faculty of the Graduate School of
the Oklahoma State University
in partial fulfillment of the requirements
for the degree of
MASTER OF SCIENCE
August, 1961

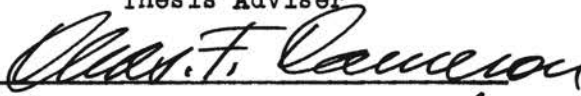
OCT 11 1961

INVESTIGATION OF INDUCTIVE ENERGY
RELATIONSHIPS IN RELAY
MAGNETIC CIRCUITS

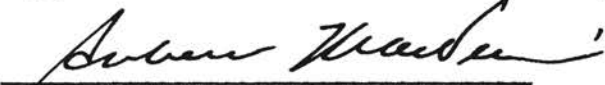
Thesis Approved:



Thesis Adviser



Dean of the Graduate School



Dean of the Graduate School

472752

PREFACE

Electronic equipment compatibility is a major reliability problem in the guided missile field today. The problem is complicated by the difficulty in performing realistic ground tests on complete systems or complete missiles.

The presence of stored inductive energy in electro-magnetic relays has caused compatibility problems such as premature erosion of switching contacts and spurious triggering of binary circuits, these malfunctions occurring during the release cycle of the relay. A better understanding of the inductive energy relationship is needed among electronic system designers. It is the objective of this paper to demonstrate a method of determining relay inductive energy storage of sufficient accuracy for practical application and which is also simple to perform.

The author wishes to acknowledge his indebtedness to Professor C. F. Cameron and Dr. D. D. Lingelbach for their guidance and assistance in performing the studies. Appreciation is also expressed to S. D. Buchanan and Carl Wade of the Douglas Aircraft Company for technical assistance in preparing instrumentation and performing measurements, to Thelma Peery and Donald Henderson of the Douglas Aircraft Company for their assistance in preparing written material and illustrations, and to my wife for her patience, her assistance in preparing the manuscript, and typing the final copy.

TABLE OF CONTENTS

Chapter	Page
I. INTRODUCTION	1
II. INDUCTANCE IN MAGNETIC CIRCUITS	4
Inductance in Linear Circuits	5
Nonlinearities in Circuits Containing Ferro Magnetic Materials	7
Sources of Nonlinearity in Inductance of Relay Magnetic Circuits	12
III. METHODS AND PROCEDURE	17
Measurement of Relay Coil Current and Search Coil Induced Voltage	20
Measurement of Coil Currents on Three Relay Specimens	27
IV. RESULTS OF MEASUREMENTS	32
Inductive Energy Calculations Using Induced Emf and Coil Current Data	32
Inductive Energy Calculations Using only Coil Current Data	40
Comparison of Inductive Energy Relationships as Determined by Four Methods	51
Inductance Studies on Three Allied MHJ-18D Relays Using Coil Current Measurements	54
V. CONCLUSIONS AND RECOMMENDATIONS	64
BIBLIOGRAPHY	66
APPENDIX	67

LIST OF TABLES

Table	Page
I. Inductive Energy Input During Closing Cycle	34
II. Inductive Energy Dissipated During Release Cycle	35
III. Inductive Energy Input with Armature Blocked Open	37
IV. Inductive Energy Input with Armature Blocked Closed	38
V. Inductive Energy Dissipated with Armature Blocked Closed	39
VI. Inductive Energy Input at 7 Volts D-C	39
VII. Inductive Energy Input as Applied Voltage is Increased from 8 to 28 Volts D-C	40
VIII. Inductive Energy Input During Closing Cycle	43
IX. Inductive Energy Dissipated During Release Cycle	44
X. Inductive Energy Input with Armature Blocked Open	46
XI. Inductive Energy Input with Armature Blocked Closed	47
XII. Inductive Energy Dissipated with Armature Blocked Closed	47
XIII. Inductive Energy Input at 7 Volts D-C	48
XIV. Inductive Energy Input as Voltage is Increased from 8 to 28 Volts D-C	48
XV. Comparison of Inductive Energy as Determined by Four Different Methods	53
XVI. Inductance of Relays During Normal Closing Cycle	56-57
XVII. Comparison of Inductances of Three Allied MHJ-18D Relays	59

LIST OF FIGURES

Figure	Page
1. Typical Magnetization Curves	9
2. Relationship Between the Relative Permeability and the Flux Density in a Cast-Iron Sample	10
3. Effect of Hysteresis in a Magnetic Material	11
4. Current vs Time in Inductance Circuits	12
5. Cutaway View Showing Search Coil Installed Inside the Relay Air Gap	19
6. Circuit Diagram of Test Circuit	20
7. Relay Characteristics During Operate Period	21
8. Relay Characteristics During Release Period	22
9. Relay Characteristics with Armature Blocked Open	23
10. Relay Characteristics with Armature Blocked Closed	24
11. Relay Characteristics with Armature Blocked Closed (Decaying Current).	25
12. Relay Characteristics with Armature Open	26
13. Relay Characteristics with Relay Coil Biased	27
14. Relay Coil Current During Normal Closing Cycle	28
15. Relay Coil Currents with Coil Voltage Increased from 17 to 28 Volts D-C	29
16. Relay Coil Currents with Coil Voltage Increased from 12 to 28 Volts D-C	29
17. Relay Coil Currents with Coil Voltage Decreased from 28 to 17 Volts D-C	30
18. Relay Coil Currents with Coil Voltage Decreased from 28 to 7 Volts D-C	31

Figure	Page
19. Inductive Energy Input during Closing Cycle	36
20. Relay Coil Current Buildup at 28 Volts D-C	42
21. Relay Coil Current Decay at 28 Volts D-C	45
22. Relay Coil Current Buildup at 7 Volts D-C	49
23. Relay Coil Current Buildup with Step Increase from 8 to 28 Volts D-C	50
24. Relay Coil Current Buildup at 28 Volts D-C	55
25. Relay Coil Currents with Step Increase from 17 to 28 Volts D-C	60
26. Relay Coil Currents with Step Increase from 12 to 28 Volts D-C	61
27. Relay Coil Currents with Step Decrease from 28 to 17 Volts D-C	62
28. Relay Coil Currents with Step Decrease from 28 to 7 Volts D-C	63

CHAPTER I

INTRODUCTION

The advancing technology required in today's guided missiles often results in electronic systems of extreme complexity. Performance requirements of electronic equipment are often beyond the present state of the art, and consequently new equipment is being continuously developed. The advancement of the state of the art usually means more complex equipment employing many more parts and newer techniques than previously used.

Unfortunately, the improvement of the reliability state of the art does not always parallel that of the performance state of the art. Reliability generally decreases as the number of individual components increases. Use of new techniques is usually accompanied by introduction of new reliability problems. Quite often the missile design engineer is in the unhappy predicament of needing greater performance capability while at the same time he must preserve or even improve reliability over that of the existing equipment.

The environments and stresses imposed upon electronic equipment employed in guided missile applications can be predicted and simulated with reasonable accuracy during ground tests. Proper use of safety factors and derating will establish test conditions that will qualify individual components for the anticipated use conditions. However, realistic tests on complete systems or on complete missiles with several systems operating in unison are much more difficult to perform.

The matter of equipment compatibility therefore becomes a major reliability problem. Study and effort in this area must be increased in order to keep pace with the reliability requirements of complex electronic systems.

Present guided missile automation and remote control requires the use of electromagnetic relays in large numbers. The presence of stored inductive energy in energized relay circuits has created serious compatibility problems. Among these are - (1) spurious triggering of binary and other digital systems by inductive voltage transients, (2) erosion of contacts switching d-c inductive loads, (3) erratic operation of relays connected in parallel.

While the presence of stored inductive energy in energized relays is recognized, the associated problems are often not fully appreciated. It is the opinion of the author that there is a need for greater awareness of these problems and a better understanding of the inductive energy relationship. It has been demonstrated that there is a close relationship between erosion of d-c switching contacts and the amount of inductive energy stored in the load (1).

The purpose of this study is to investigate methods for determining the inductive energy storage in relay magnetic circuits. This study will be directed toward demonstrating practical methods of reasonable accuracy that can be understood and applied by the average system designer without the help of a relay expert.

With few exceptions, the relays used in guided missiles are hermetically sealed relays. The advantages of sealed relays over open type relays necessitates their use in such applications. However, some of the measurements easily made on open type relays are impossible to make on hermetically sealed relays without disturbing the construction

of the relay. It is hoped that this study will demonstrate methods that can be conveniently applied to hermetically sealed relays with sufficient accuracy for good design practice.

CHAPTER II

INDUCTANCE IN MAGNETIC CIRCUITS

A discussion of the characteristics of relay inductance is in order as a basis for the investigation of inductive energy relationships in electromagnetic relays.

Self-induction is defined as the property of a circuit that causes an emf to be induced in the circuit by a change of the current (2). The coefficient of self-induction, called the inductance, is represented by the symbol L . The emf generated in an inductive circuit is defined by the formula

$$e \text{ (volts)} = -L \text{ (henries)} \frac{di}{dt} \text{ (amperes/second)}$$

where e is the instantaneous emf and the negative sign indicates that the direction of the emf opposes the change of current in the circuit.

Another definition of induced emf is the relationship

$$e = -\frac{d\lambda}{dt}$$

where e is the instantaneous emf in volts and $d\lambda/dt$ is the rate of change of flux linkages in weber turns per second. Equating

$$-\frac{d\lambda}{dt} = -L \frac{di}{dt}$$

gives the relationship

$$L \text{ (henries)} = \frac{d\lambda}{di} \text{ (Weber turns/ampere)}.$$

Inductance is thereby defined as the rate of change of flux linkage with respect to the current.

For most electric circuits, $d\lambda = N d\phi$, so that

$$L \text{ (henries)} = N \frac{d\phi}{di}$$

where N equals the number of turns in the inductance and $d\phi/di$ is the rate of change of flux with respect to current in webers per ampere. This relationship can be considered as a general relationship since the expression $d\phi/di$ accounts for constant as well as varying rates of change of flux with current.

INDUCTANCE IN LINEAR CIRCUITS

In the special case of a constant $d\phi/di$

$$L = N \frac{\phi}{i}$$

The expression

$$e = -L \frac{di}{dt}$$

is particularly useful in this case since di/dt can be easily observed on an oscilloscope trace. The inductance L is constant since the relationship ϕ/i is constant throughout the current range. This situation occurs in a circuit surrounded by nonmagnetic materials because the flux linking the circuit is directly proportional to the current in the circuit (2). Calculations for circuits with constant inductance are facilitated by the inductance concept. A constant inductance is also known as a linear inductance, and systems containing only linear elements are called linear systems.

Since the emf generated in an inductive circuit opposes the change of current in the circuit, the effect of inductance is to delay the change of the current to a steady state value when the applied voltage is changed. In a d-c circuit containing only resistance and inductance

the current is expressed as

$$i(t) = I \left(1 - e^{-\frac{Rt}{L}} \right)$$

where $i(t)$ equals instantaneous current in amperes, I is the steady state current in amperes, R is the resistance of the circuit in ohms, L is the inductance in henries, and t is the time in seconds after change of applied voltage. The time constant of a linear RL circuit is defined as

$$T' = \frac{L}{R}$$

where T' is the time in seconds at which the current has changed by 63.2% from its original to its steady state value. Rudenberg (3) discusses these relationships on pp. 7-13.

The energy input to an electrical circuit during an interval of time T is given by

$$W \text{ (watts)} = \int_0^T Vi \, dt$$

where V and i are instantaneous values of voltage and current in volts and amps, respectively, and T is the time of energy input in seconds. In the case of d-c current flow in an inductance the period T is the transient period during which current is changing since no emf is produced in the inductance when the current is at the steady state value. The energy input to a linear inductance can be expressed as

$$W_L = \int_0^T L \frac{di}{dt} \cdot i \, dt = \int_0^I Li \, di$$

since $V_L = L \frac{di}{dt}$.

Integration of the above gives the relationship

$$W_L = \frac{Li^2}{2} \text{ joules.}$$

It is not necessary to know how the current varied with time in the above expression so long as L is constant, and after the current has reached the steady-state value there is no further energy input to the circuit (2).

The energy input to an inductance is not dissipated as heat as in the case of a resistor. Therefore, the energy remains stored in the inductance and is ready to be released when the applied voltage is removed from the circuit.

NONLINEARITIES IN CIRCUITS CONTAINING FERRO-MAGNETIC MATERIALS

As shown by the preceding discussion, the calculation of the inductive energy stored in a energized linear circuit is a relatively simple matter, requiring only a knowledge of the amount of the inductance and the steady state value of current in the circuit. It would indeed be a useful relationship for any circuit to which it could be legitimately applied since very little time and rigor are involved in this calculation. Unfortunately, many magnetic circuits are nonlinear, and the $LI^2/2$ relationship does not hold in these cases since $i(t)$ does not see a constant inductance for all values of i .

Nonlinear inductance is found in iron-core transformers. Nonlinearities are also present, and from more sources, in energy conversion devices with movable armatures. Electromagnetic relays are in this class along with solenoids, motors, and generators.

A magnetic circuit, i.e. a circuit containing a closed flux path is analogous to an electric circuit containing a closed current path. The driving force, comparable to the emf of an electric circuit, is the magnetomotive force (mmf) resulting from the flow of current through a wire or the turns of a coil. Mmf is usually expressed in ampere-turns.

The flux resulting from the application of mmf to a magnetic circuit is analogous to current in an electric circuit. The unit of flux is the weber which is equal to 10^8 lines of flux.

In much the same manner that current is opposed by the resistance of an electric circuit the flux is opposed by the reluctance of a magnetic circuit. The reluctance of a specimen of material of given length and cross section area is inversely proportional to a property known as the permeability (μ) of the material. Consequently, it is seen that a material of relatively high permeability will have a low reluctance and will therefore provide a good path for the flux.

The relative permeability of a vacuum has been arbitrarily assigned as unity. Air and most other materials also have relative permeability of unity, and are called non-magnetic materials. Magnetic materials, such as iron, steel, cobalt, and nickel may have a relative permeability much greater than unity (2).

Magnetization curves for various types of magnetic materials may be determined by measurements. A discussion of these methods is beyond the scope of this paper but they are discussed by Mueller (2) on pp. 263-268. Typical magnetization curves for sheet steel and cast iron are shown in Figure 1.

The flux density (B) is plotted versus the magnetic potential gradient (H). Flux density (B) is equal to the total flux (ϕ) divided by the cross-sectional area of the material, and magnetic potential gradient (H) is the mmf per unit length of the flux path. The relationship between flux density and magnetic potential gradient is shown by

$$B = 4\pi \times 10^{-7} \mu H$$

where μ is the relative permeability of the material in the magnetic conductor. In reality, Figure 1 could be called a ϕ vs I curve since

the flux (ϕ) and current (I) are the variables in B and H respectively.

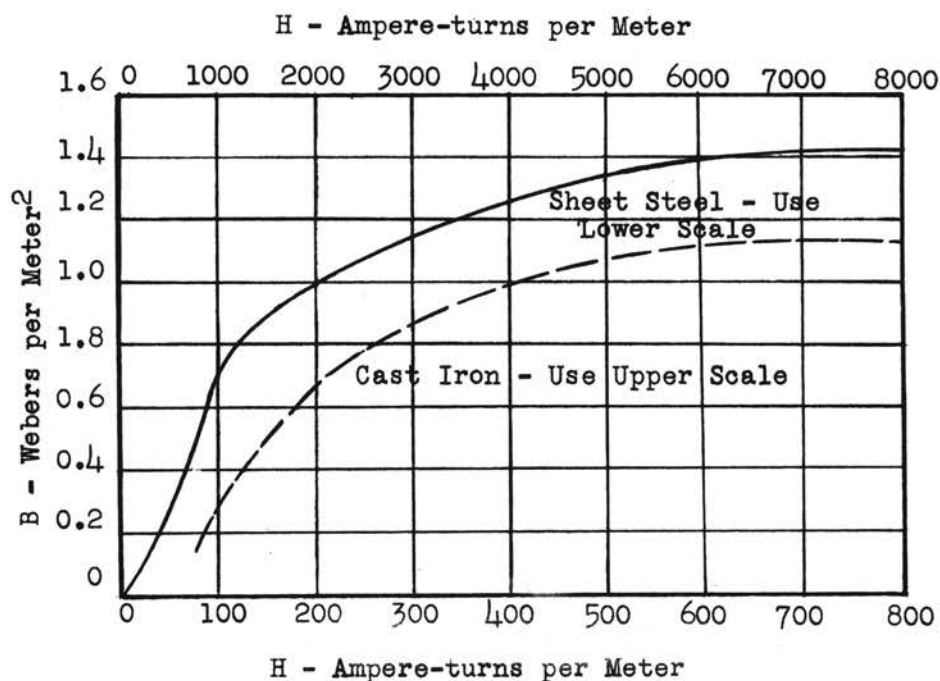


FIGURE I - TYPICAL MAGNETIZATION CURVES

As seen in Figure 1, the flux density of steel is not directly proportional to the magnetic potential gradient of the circuit. For steel and other magnetic materials the relative permeability is not constant but is a function of the flux density (2). The relationship between relative permeability and flux density in a cast iron sample is shown in Figure 2.

The varying slope of the magnetization curves illustrates the fact that μ is varying. A constant μ would result in a linear B-H curve as shown by the formula on page 8. At low flux density the slope of the line increases with H. There is then a region of medium flux density in which the slope of the curve is nearly constant. At high flux density the slope decreases with increasing H. It is in this region that saturation occurs so that the rate of increase of flux with current is growing progressively smaller (2).

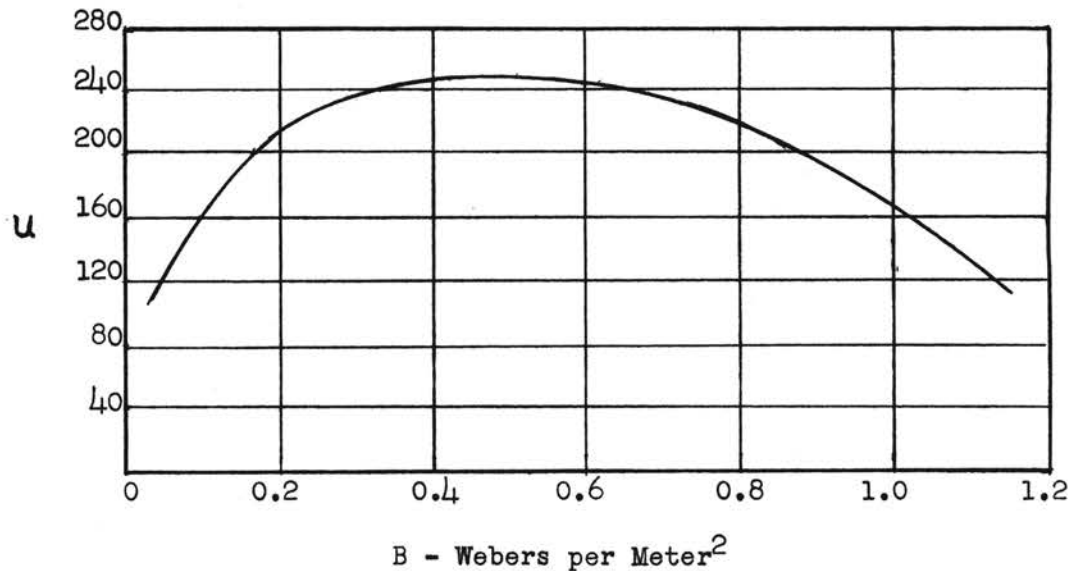


FIGURE 2 - RELATIONSHIP BETWEEN THE RELATIVE PERMEABILITY AND THE FLUX DENSITY IN A CAST-IRON SAMPLE

Recalling the relationship

$$L = N \frac{d\phi}{di}$$

it is seen that the inductance of a circuit containing magnetic materials is not constant for all values of L . At low flux densities, $d\phi/di$ will be increasing, may then be fairly constant for a small range of values, and will finally start decreasing as saturation is reached. Thus is illustrated the source of one of the nonlinearities in the inductance of a magnetic circuit.

The magnetization or saturation curve of a specimen of magnetic material may also vary due to previous magnetic history of the specimen. If an mmf has previously been applied to a specimen and residual magnetism is present, the curve will not start at B equal zero but at the flux density corresponding to the level of residual flux present. The presence of residual flux is called the hysteresis effect and is caused by the

change in permeability at varying flux densities (2). The effect of hysteresis is shown in Figure 3.

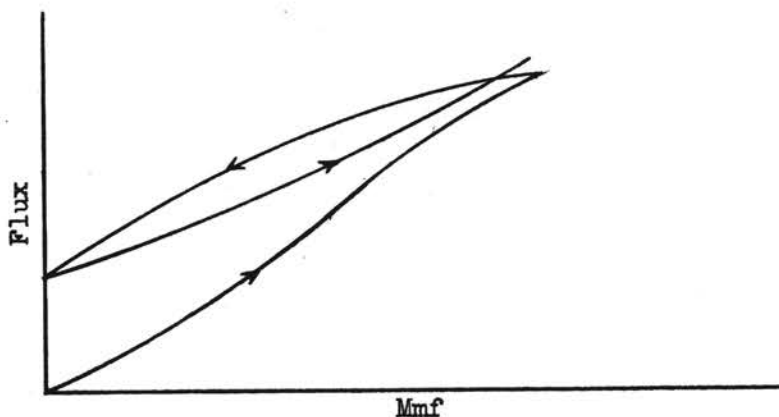


FIGURE 3 - EFFECT OF HYSTERESIS
IN A MAGNETIC MATERIAL

The effect of hysteresis on the inductance, $N d\phi/di$, is also illustrated by Figure 3. However, it is found that after several cycles of varying current in the exciting coil between two given values the residual flux remains essentially constant and the flux and current values settle into a definite cycle. This is known as the hysteresis loop (2).

Most iron-core inductors have an air gap in the magnetic material, either to obtain some specific operating characteristic or to facilitate the construction of the core. The air gap has a profound influence on the saturation curve of the magnetic current. It has been shown that the presence of an air gap causes the residual flux to be less than if the air gap were not present. If the length of an air gap is changed between magnetization cycles, the saturation curves will be different. In one case, an air gap of only 0.005 meters in a steel specimen resulted in an almost linear B-H curve with very little hysteresis effect (2).

In summary, the major sources of nonlinearity in magnetic circuits are:

1. Saturation in magnetic materials
2. Residual magnetism
3. Air gaps

The growth of current with time in a nonlinear inductor is compared to that of a linear inductor in Figure 4.

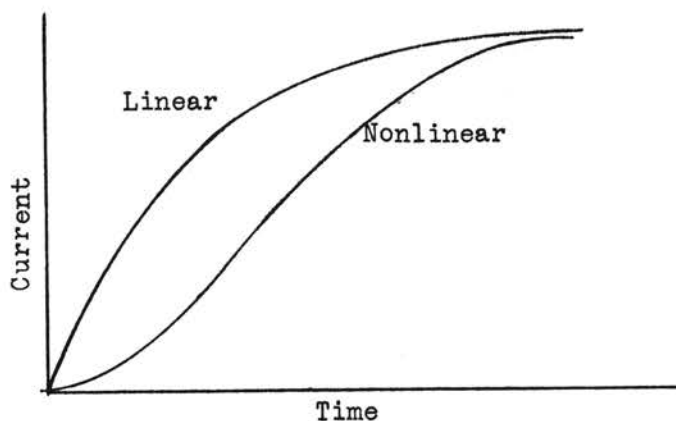


FIGURE 4 - CURRENT VS TIME IN INDUCTANCE CIRCUITS

The energy relationship, $W_L = LI^2/2$, is not exact in a nonlinear inductance since L is not constant for all $i(t)$. When $V_L(t)$ and $i(t)$ are known the energy, W_L , may be approximated by a summation of $V_L i \times \Delta t$ for small increments of time as in

$$W_L = \int_0^T V_L i \, dt.$$

SOURCES OF NONLINEARITY IN INDUCTANCE OF RELAY MAGNETIC CIRCUITS

The three sources of nonlinearity discussed in the preceding paragraph - (1) saturation, (2) residual flux, (3) air gap - are all present in electromagnetic relays. However, since a relay is a

particular type of electro-mechanical device, the effect of each of these sources warrants further discussion.

Transients are involved in both the electrical and mechanical systems of a relay. The electrical transient occurs when there is a change in the applied voltage resulting in a corresponding change in the relay coil current. Normally this is a change from zero voltage to a specified level of operating voltage or vice-versa. As seen in Figure 4, a step increase or decrease in applied voltage is not accompanied by a simultaneous current change but instead there is a period of time delay in the change of the current to a steady state value. The mechanical transient occurs during, but not coincident with, the electrical transient. In other words, the period of time involved in the mechanical transient is not the same as the period of the electrical transient but is usually much less.

The mechanical transient period is that period during which the armature moves from the open position to the final closed position or vice-versa. This includes the bounce time after the initial armature closure. After application of voltage there is a period of time before enough force is developed to overcome the friction of the movable armature and tension of the armature restraining spring. Armature closure usually is completed very rapidly after the initial movement, and the coil current continues to build up to a steady state value after closure.

For convenience, the three states of the armature during the current transient can be called the open state, the transition state, and the closed state. The magnetic relations during the three states are different and must be treated individually. The classic expression for induced emf

$$e = N \frac{d\phi}{dt}$$

is descriptive of the open and closed states when the differences in $d\phi/dt$ for the two states and within the periods of the two states are remembered. Although this expression is also correct for the transition state, it is not sufficient in this form to really describe what is occurring in the magnetic circuit.

For the open and closed states, $d\phi/dt$ may be expressed as

$$\frac{d\phi}{dt} = \frac{d\phi}{di} \cdot \frac{di}{dt}$$

since the current is the variable that controls the rate of change of flux. During the transition state, there is another variable introduced which is the change of length of the air gap. This variable may be expressed as dx/dt . Since the flux is now influenced by both the current and the air gap, $d\phi/dt$ may be expressed as

$$\frac{d\phi}{dt} = \frac{\partial \phi}{\partial i} \cdot \frac{di}{dt} + \frac{\partial \phi}{\partial x} \cdot \frac{dx}{dt} \quad (4).$$

During the open state the length of the air gap is usually sufficient to limit the effect of saturation of the armature on the overall reluctance of the flux path. Magnetization curves plotted at varying air gap lengths indicate that the ϕ vs i relationship is almost linear with the armature open (5). The inductance during this period is usually considered to be constant (6).

The change in the ϕ vs i relationship for the different values of air gap length may be illustrated by measurements taken with the armature blocked at various air gap lengths between the open and closed position. If the correlation between relay current and armature motion during the transition state is also known, the ϕ vs i relationship may be determined by superimposing the current value on each ϕ vs i curve for the various gap lengths and connecting the points. An abrupt

change will occur in this relationship when the air gap length becomes zero, i.e. the end of the transition state (5). Since the change of current level and air gap length both contribute to the nonlinearity of the magnetic circuit during the transition state, the inductance characteristic is most difficult to assess during this state.

After armature closure, saturation will occur rapidly, and its effect will be much more noticeable than before. Since an appreciable amount of current was flowing in the coil at the time of closure, it is likely that the range of mmf for essentially constant reluctance as discussed on p. 9 is largely expended at this time and saturation occurs almost immediately. During release the armature holds in until the current decreases to a level much less than that required to close the armature initially. Therefore the saturation effect is greater during the release cycle than during the closing cycle.

The effect of residual flux is present in relays as in all circuits containing magnetic materials. However, this effect is usually constant after the first few cycles since operating voltages are normally at one specified level and vary very little. One noticeable effect of residual flux or hysteresis is the difference in inductance at a given current level for the pull-in and release operations.

The following observations are presented as a summary of the effects of the various factors influencing the inductance of a relay magnetic circuit:

1. Since the reluctance of the flux path is greatly influenced by the length of the air gap, the relay inductance is partially determined by the position of the armature. A different value of inductance would be expected for each of the three states of armature operation.

2. Since the reluctance varies with the flux density in magnetic materials, a different value of inductance would be expected at each current level. This effect is greatest when the armature is closed and is negligible with the armature open due to the large reluctance of the air gap.
3. The effect of residual flux in the circuit is essentially constant after a few cycles of operation at a given voltage level.
4. Considerable difference is expected in the inductive effect of the relay circuit during the operate and release periods. This is partially due to the hysteresis effect and partially due to the difference in the time that the armature is closed during the two cycles.

CHAPTER III

METHODS AND PROCEDURES

Two methods were used during this study to investigate the storage of inductive energy in the relay magnetic circuit. Most of the effort was concentrated on the periods when the armature was in the open and the closed positions.

The reasons for the relatively small amount of study during the transition state of the armature are as follows:

1. Processing and interpretation of current and voltage data during the transition state is much more tedious and time consuming than during the other two states.
2. Since inductive energy is actually being delivered to the mechanical system of the relay during the transition state, the net amount of inductive energy storage during the transition state was believed to be negligible.

Therefore, the benefits derived from the study of data obtained during the transition period did not appear to warrant the expenditure of the time and effort required.

The first method of determining energy storage was the application of measured data to the relationship

$$W_L = \int_0^T V_L i \, dt.$$

Measurements were taken to determine the relay coil induced emf (V_L) and current (i) vs time during the transient periods. The above relationship was then modified as

$$W_L = \sum_1^n P_n \Delta T_n$$

Where P_n are average values of power ($V_L \times i$) during the periods (ΔT_n) and $\sum \Delta T_n$ is equal to the total transient period. The various ΔT_n 's were chosen to minimize the errors incurred due to the lack of constant slope of the traces of current and/or voltage vs time. The accuracy of this method is limited only by the accuracy of the test instrumentation and the skill of the data analyst.

The second method employed only the coil current data obtained for the first method. The relationship

$$W_L = \frac{LI^2}{2}$$

was modified to give

$$W = \sum_1^n \frac{L_n}{2} [I_2^2 - I_1^2] \Delta T_n$$

where L_n is the average L during ΔT_n and I_1 and I_2 are initial and final values, respectively, of relay coil current during the corresponding ΔT_n . The method of determining L_n is given in the appendix. The accuracy of this method of energy calculation was determined by comparison with the corresponding results of the first method.

Data for these two methods were obtained from measurements taken on one Allied Control Type MHJ-18D relay. Measurements were taken at several different conditions of the armature and various values of applied voltage.

In addition to the data discussed above, measurements of relay coil current vs time were taken simultaneously on three Allied MHJ-18D relays. These data were also taken at several different armature conditions and voltage levels. The purpose of these measurements was to observe the difference in inductance values obtained by this method

for several relay specimens of the same type.

A search coil was used to determine the emf induced in the relay coil. The search coil consisted of 72 turns of fine wire placed in the center of the relay coil spool adjacent to the air gap.

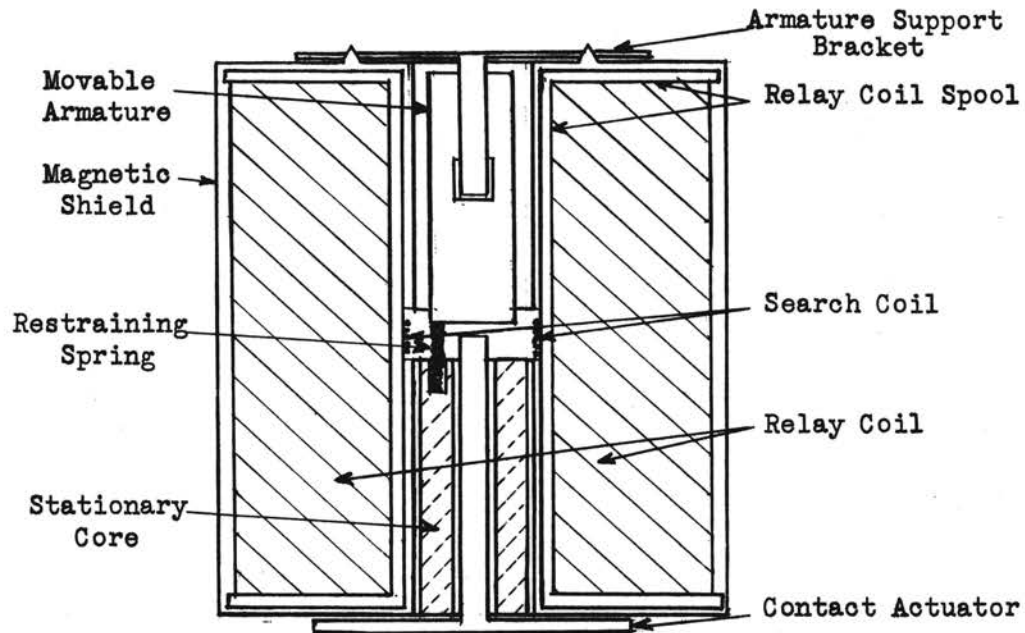


FIGURE 5 - CUT AWAY VIEW SHOWING SEARCH COIL INSTALLED INSIDE THE RELAY AIR GAP

The search coil voltage was recorded on an oscilloscope trace. Since the high impedance of the oscilloscope limits the current in the search coil to a negligible value, the search coil voltage is a satisfactory measure of the induced emf in the relay coil. The relay coil induced emf was calculated by the relationship

$$e(\text{relay coil}) = \frac{1}{K_c} \frac{N(\text{relay coil})}{N(\text{search coil})} e(\text{search coil}).$$

K_c is the coefficient of coupling between the two coils and was determined by measurements of the search coil voltage with a low value of a-c voltage. The relay coil current was determined by

recording the voltage drop across a resistance in series with the relay coil. The oscilloscope was then calibrated in milliamperes by dividing the millivolt indication by the resistance of the series resistor. The search coil voltage and relay coil current traces on the oscilloscope were photographed by a Polaroid camera attached to the oscilloscope screen. A Textronix Type 502 Dual Beam oscilloscope was used to simultaneously record the two traces. The diagram of the test circuit is shown in Figure 6.

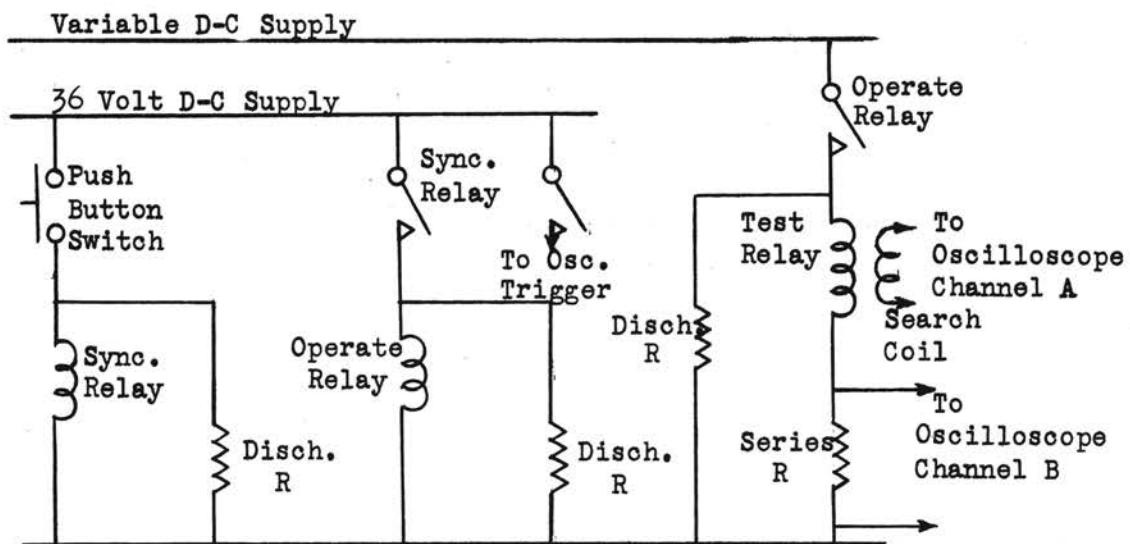


FIGURE 6 - CIRCUIT DIAGRAM OF TEST CIRCUIT

MEASUREMENTS OF RELAY COIL CURRENT AND SEARCH
COIL INDUCED VOLTAGE

Seven different procedures were used for measuring these data. There was a dual purpose for using more than one procedure. First, it was considered desirable to investigate the difference in the inductive effect of the relay circuit with different positions of the armature. Second, and more important, a procedure for determining inductive energy with reasonable accuracy, using only the coil current vs time trace,

was desired. This is one of the primary objectives of the investigation since the current trace is easily obtained for an hermetically sealed relay. Investigation by several different procedures affords an opportunity for comparison to determine the most accurate procedure. For convenience, the various procedures are listed in chronological order and discussed:

Procedure Number One

The relay was cycled on and off several times to obtain a constant hysteresis effect. Then, with the relay de-energized, a potential of 28 volts d-c was applied and the current and voltage traces obtained, as shown in Figure 7.

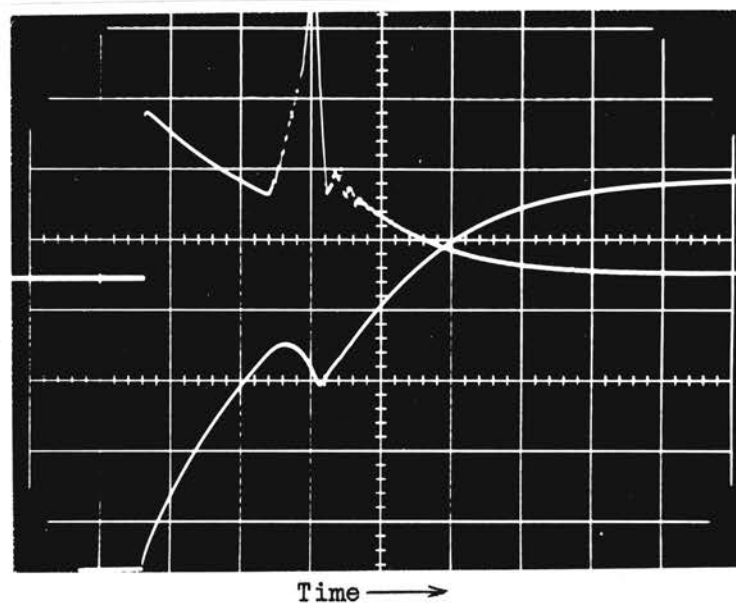


FIGURE 7 - RELAY CHARACTERISTICS DURING
OPERATE PERIOD

Relay coil voltage - 28 volts d-c
 Upper trace - search coil voltage
 Sensitivity - 100 mv/cm
 Lower trace - relay coil current
 Sensitivity - 22 ma/cm
 Time scale - 2.5 millisec/cm

Procedure Number Two

The procedure was the same as number one except that the relay was energized at 28 volts d-c and the traces were recorded during the release period. These traces are shown in Figure 8. The connections from the search coil to the oscilloscope were reversed for the sake of convenience since otherwise the polarity of the voltage trace would appear opposite to that shown. The relay coil was discharged through a 1000 ohm resistor.

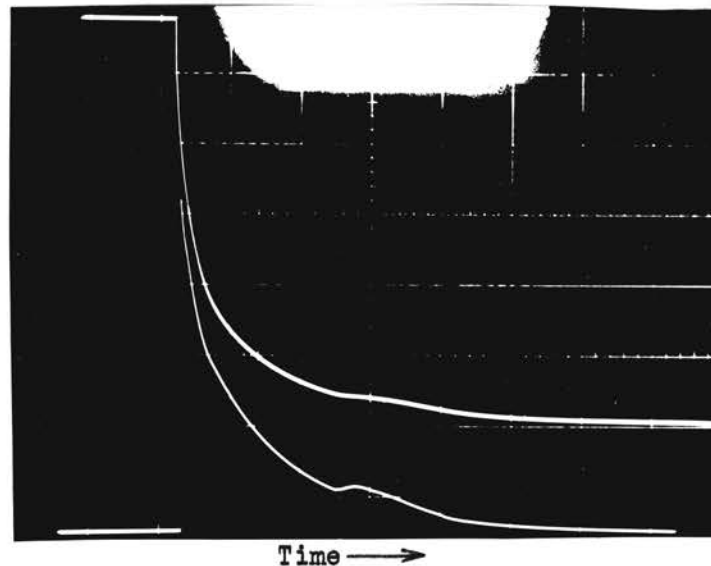


FIGURE 8 - RELAY CHARACTERISTICS DURING
RELEASE PERIOD

Relay coil voltage - 28 volts d-c
 Upper trace - Relay coil current
 Sensitivity - 22 ma/cm
 Lower trace - Search coil voltage
 Sensitivity 0.2 v/cm
 Time scale - 2 millisec/cm

Procedure Number Three

The armature of the relay was blocked in the open position. A potential of 28 volts d-c was applied and the traces of voltage and current recorded. Due to improper positioning of the current trace on the oscilloscope screen, a very small portion of the trace at the beginning of the period was not recorded (Figure 9). This necessitated

a slight extrapolation.

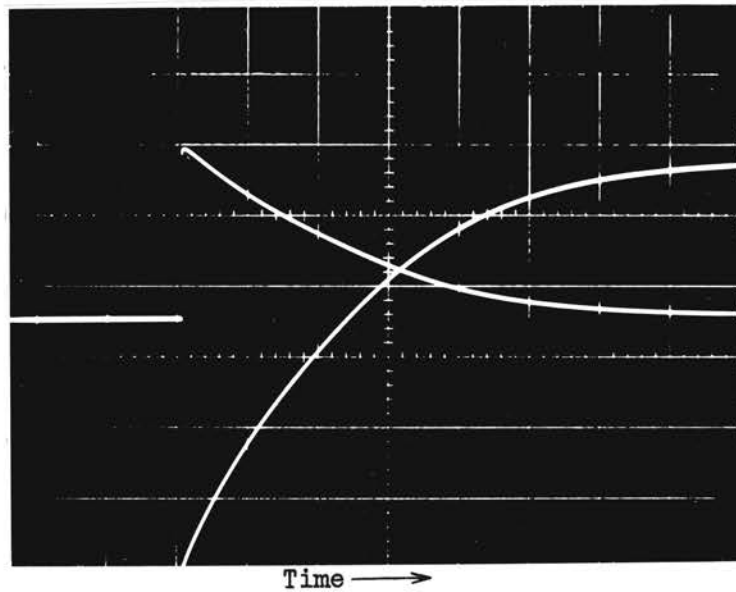


FIGURE 9 - RELAY CHARACTERISTICS WITH
ARMATURE BLOCKED OPEN

Relay coil voltage - 28 volts d-c
 Upper trace - Search coil voltage
 Sensitivity - 100 mv/cm
 Lower trace - Relay coil current
 Sensitivity - 22 ma/cm
 Time scale - 2.5 millisec/cm

Procedure Number Four

This was the same as procedure three except that the armature was blocked in the closed position. The initial portion of the current trace was also missed in this photograph (Figure 10).

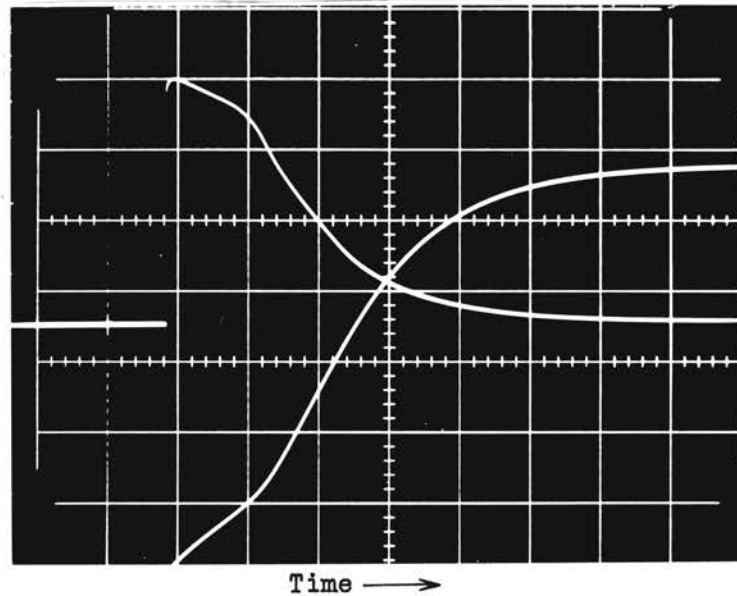


FIGURE 10 - RELAY CHARACTERISTICS WITH
ARMATURE BLOCKED CLOSED

Relay coil voltage - 28 volts d-c
 Upper trace - Search coil voltage
 Sensitivity - 100 mv/cm
 Lower trace - Relay coil current
 Sensitivity - 22 ma/cm
 Time scale - 2.5 millisecc/cm

Procedure Number Five

The relay was energized with 28 volts d-c with the armature blocked closed. The voltage was removed from the relay and the current and voltage traces recorded. The relay was discharged through a 1000 ohm resistor (Figure 11).

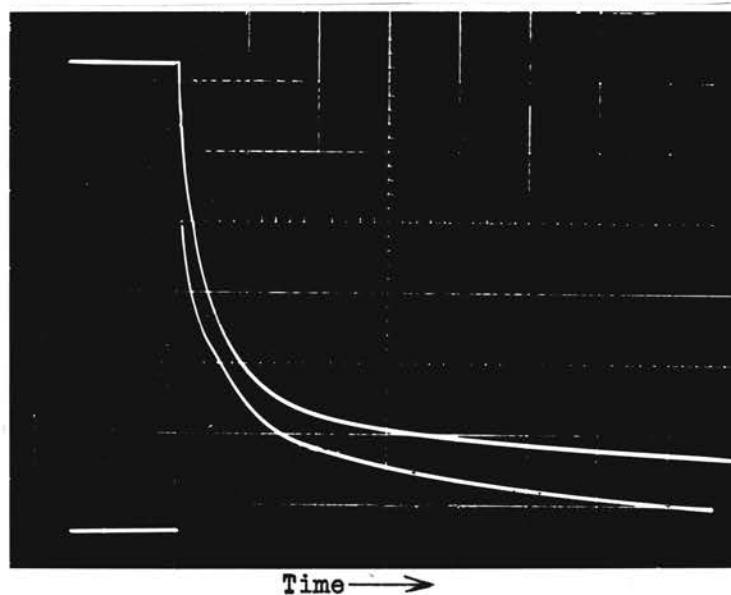


FIGURE 11 - RELAY CHARACTERISTICS WITH ARMATURE
BLOCKED CLOSED (DECAYING CURRENT)

Relay coil voltage - 28 volts d-c
 Upper trace - Relay coil current
 Sensitivity - 22 ma/cm
 Lower trace - Search coil voltage
 Sensitivity - 0.2 v/cm
 Time scale - 1 millisecc/cm

Procedure Number Six

The relay was energized with 7 volts d-c which is just below the level at which the armature starts to close. The current and voltage traces are shown in Figure 12.

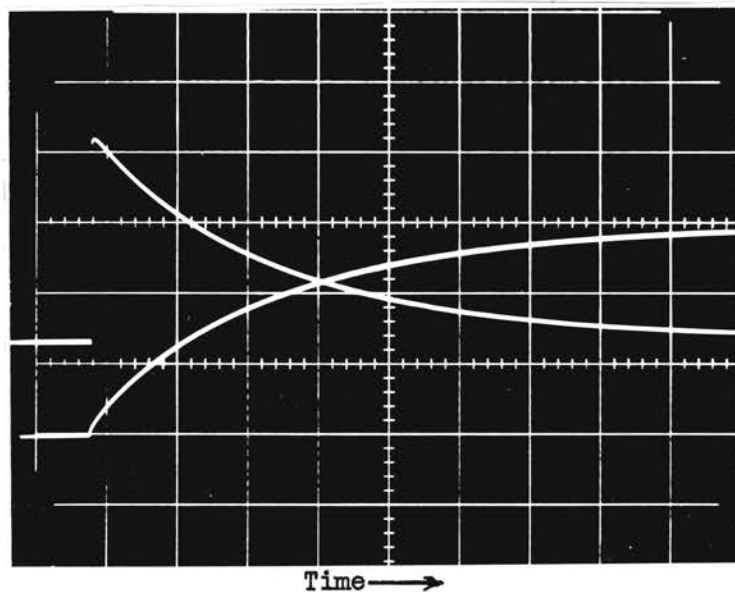


FIGURE 12 - RELAY CHARACTERISTICS WITH
ARMATURE OPEN

Relay coil voltage - 7 volts d-c
 Upper trace - Search coil voltage
 Sensitivity - 20 mv/cm
 Lower trace - Relay coil current
 Sensitivity - 11 ma/cm
 Time scale - 2.5 millisec/cm

Procedure Number Seven

A bias voltage of 8 volts d-c was applied to the relay coil. This is just above the voltage level required to close the armature. The coil voltage was then increased to 28 volts d-c and the current and voltage traces recorded (Figure 13).

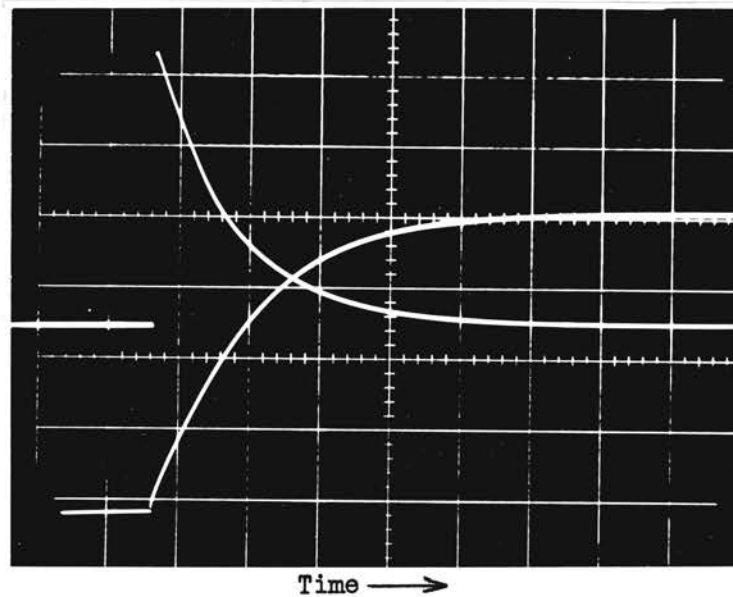


FIGURE 13 - RELAY CHARACTERISTICS WITH
RELAY COIL BIASED

Relay coil voltage - Biased at 8 volts d-c
Step increase to 28 volts d-c
Upper trace - Search coil voltage
Sensitivity - 50 mv/cm
Lower trace - Relay coil current
Sensitivity - 22 ma/cm
Time scale - 2.5 millisecc/cm

MEASUREMENTS OF COIL CURRENTS OF THREE RELAY SPECIMENS

Five different procedures were used during these measurements in order to compare the inductances of the three relay specimens under several conditions. All of the test specimens were Allied Control Type MHJ-18D relays. These procedures will be referred to as procedures 8 through 12 in order to distinguish between those of the previous series of measurements:

Procedure Number Eight

With the relays de-energized, a potential of 28 volts d-c was applied to the relay coils, and the current traces were recorded sequentially on the same photograph. These data are shown in Figure 14.

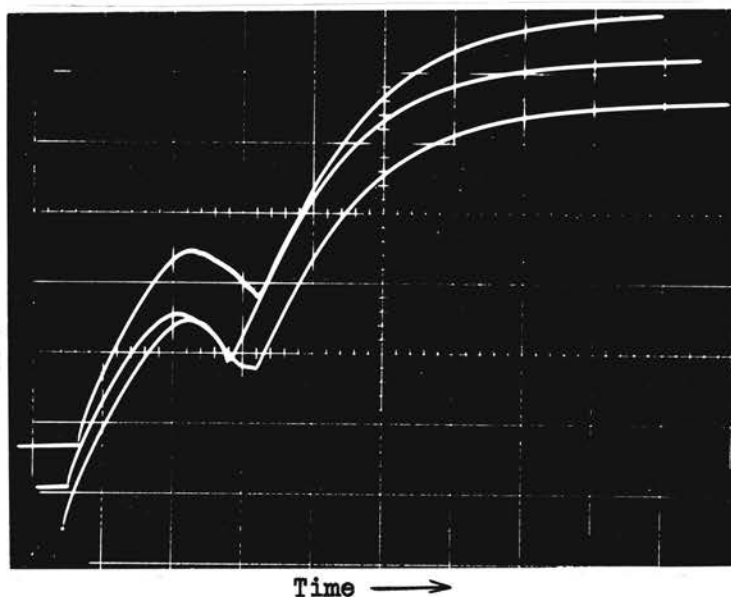


FIGURE 14 - RELAY COIL CURRENTS DURING
NORMAL CLOSING CYCLE

Relay coil voltage - 28 volts d-c
Current scale - 20 ma/cm
Time scale - 2.5 millisecc/cm

Procedure Number Nine

The relay coils were biased at 17 volts d-c and the current traces recorded as the applied voltage was increased from 17 to 28 volts by a step function (Figure 15).

Procedure Number Ten

The relay coils were biased at 12 volts d-c and the current traces recorded as the applied voltage was increased from 12 to 28 volts by a step function (Figure 16).

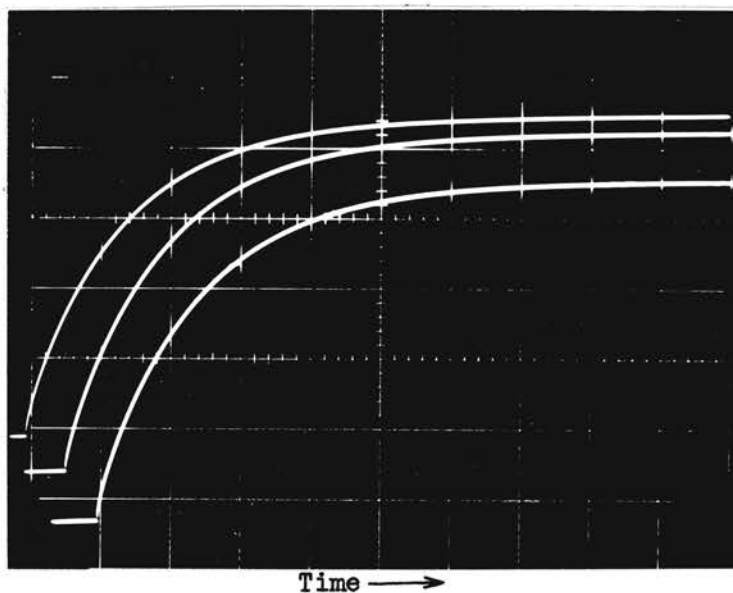


FIGURE 15 - RELAY COIL CURRENTS WITH COIL
VOLTAGE INCREASED FROM
17 TO 28 VOLTS D-C

Current Scale - 10 ma/cm
Time scale - 2 millisecc/cm

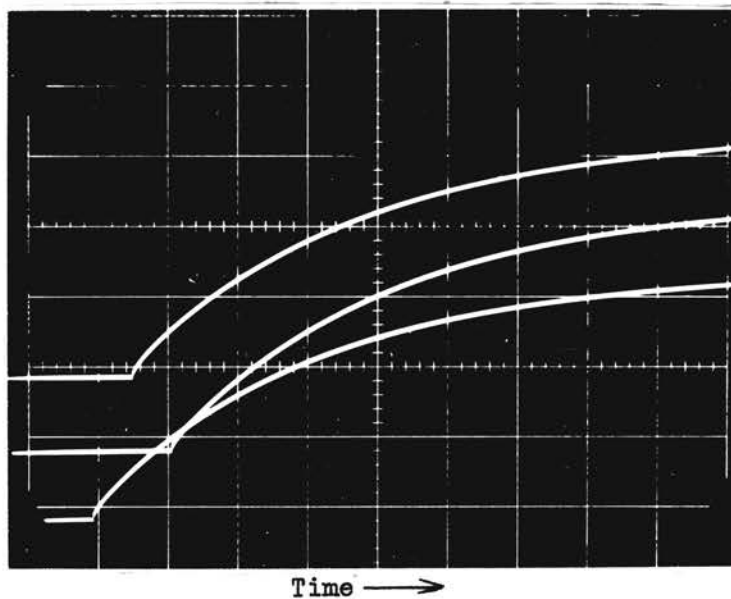


FIGURE 16 - RELAY COIL CURRENTS WITH COIL
VOLTAGE INCREASED FROM
12 TO 28 VOLTS D-C

Current scale - 20 ma/cm
Time scale - 1 millisecc/cm

Procedure Number Eleven

The relay coils were biased at 28 volts d-c and the current traces recorded as a step function decrease to 17 volts d-c was applied (Figure 17).

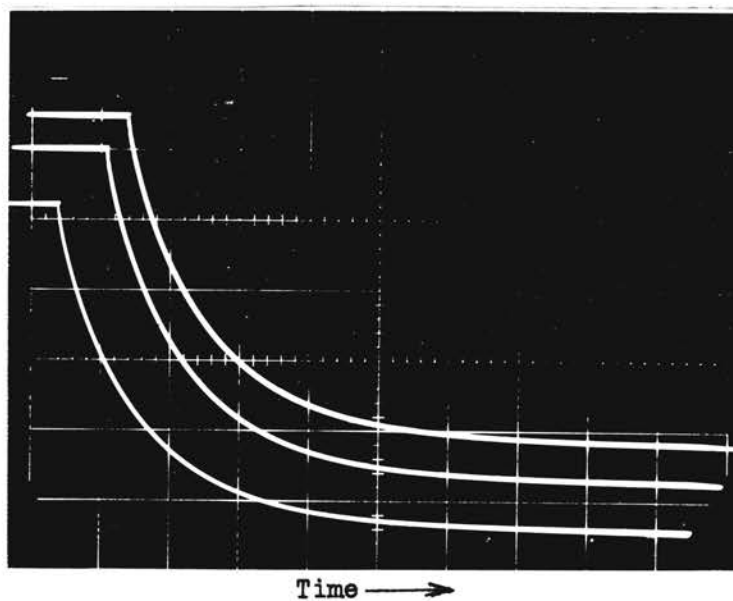


FIGURE 17 - RELAY COIL CURRENTS WITH COIL
VOLTAGE DECREASED FROM
28 to 17 VOLTS D-C

Current scale - 10 ma/cm
Time scale - 1 millisecc/cm

Procedure Number Twelve

The relay coils were biased at 28 volts d-c and the current traces recorded as a step function decrease to 7 volts was applied. The current traces are shown in Figure 18.

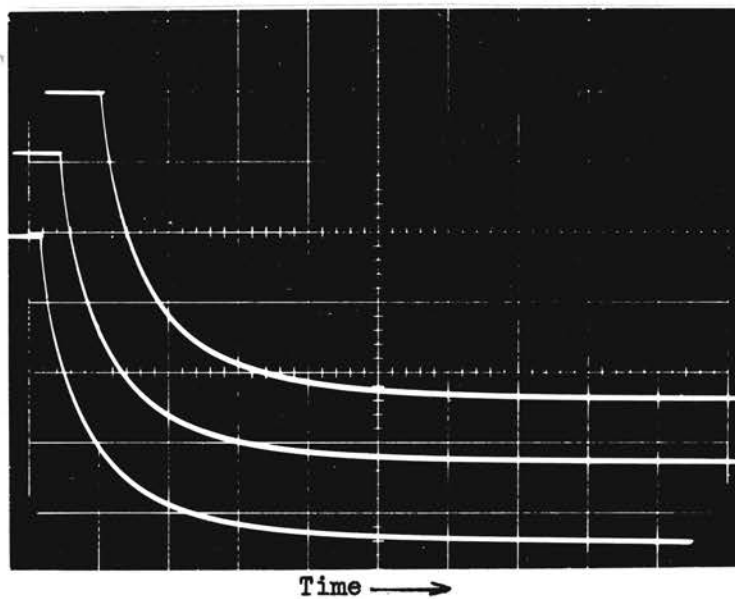


FIGURE 18 - RELAY COIL CURRENTS WITH COIL
VOLTAGE DECREASED FROM
28 to 7 VOLTS D-C

Current scale - 20 ma/cm
Time scale - 1 millisecc/cm

The data from these measurements are discussed in chapter 4. The circuit used for Procedure 7 and Procedure 9 through 12 is shown in the appendix.

CHAPTER IV

RESULTS OF MEASUREMENTS

The data obtained in the measurements discussed in Chapter III are presented in this chapter. The data of Figures 7 through 18 were tabulated and used to calculate the inductive energy storage or dissipation by four different methods. The data of Figures 14 through 18 were used to compare the inductance of three relays of the same type under several conditions.

INDUCTIVE ENERGY CALCULATIONS USING INDUCED EMF

AND COIL CURRENT DATA

This is theoretically an absolute method for determining the inductive energy and is limited in accuracy only by the precision of the measurements and of the data processing. Unfortunately this method is rather rigorous and requires special instrumentation as discussed on p. 19. It is certainly inconvenient for measurements on hermetically sealed relays. However, this method was considered desirable for this study since it can be used as a standard by which the accuracy of the other methods can be compared.

The values of search coil voltage (e_s) and relay coil current (i) vs time from Figures 7 through 18 were tabulated. The relay coil induced emf (e_r) was determined by the relationship

$$e_r = \frac{e_s \times N_R}{K_C}$$

where N_R is the turns ratio between the relay coil and the search coil and K_C is the coefficient of coupling between the two coils. The method by which K_C was determined is discussed in appendix.

The power input was calculated from

$$P \text{ (watts)} = e_r \text{ (volts)} \times i \text{ (amps)}$$

where P , e_r , and i are instantaneous values. Finally, the inductive energy was determined by

$$W_L \text{ (joules)} = \sum P_{\text{ave}} \text{ (watts)} \times \Delta t \text{ (seconds)}$$

where P_{ave} is the average power input during Δt . The various Δt 's were chosen carefully in small increments to obtain good accuracy.

The data of Figure 7 are listed in Table I. Sample calculations for lines 1 and 10 of this data are shown below. Two sets of sample calculations are shown because of the different coefficients of coupling (K_C) of the relay with the armature open and closed.

Sample Calculations

Line 1 - Armature open, $t = 1$ millisecond

$$K_C = 0.495, e_s = 204 \text{ millivolts}, i = 22.88 \text{ milliamps}$$

$$N_R = \frac{\text{Relay coil turns}}{\text{Search coil turns}} = \frac{4450}{72} = 61.8$$

$$e_r = \frac{e_s \times N_R}{K_C} = \frac{204 \times 10^{-3} \times 61.8}{.495} = 25.5 \text{ volts}$$

$$P = e_r \times i = 25.5 \times 22.88 = 583.5 \text{ milliwatts}$$

$$\begin{aligned} \Delta W &= \int P \, dt = P_{\text{ave}} \int_0^1 \times \Delta t \Big|_0^1 = \frac{583.5 \times 1 \times 10^{-3}}{2} \\ &= .292 \text{ millijoules} \end{aligned}$$

Line 10 - Armature closed, $t = 7.5$ milliseconds

$$K_c = 0.7, e_s = 114 \text{ millivolts}, i = 71.28 \text{ milliamps}$$

$$N_R = 61.8$$

$$e_r = \frac{e_s \times N_R}{K_c} = \frac{114 \times 10^{-3} \times 61.8}{0.7} = 10.0 \text{ volts}$$

$$P = e_r \times i = 10.1 \times 71.28 = 719.9 \text{ milliwatts}$$

$$\Delta W = P_{\text{ave}} \times \Delta t = \frac{719.9 - 894.5}{2} \times 1 \times 10^{-3}$$

$$= .808 \text{ millijoules}$$

TABLE I

INDUCTIVE ENERGY INPUT DURING CLOSING CYCLE

Time millisec	e_s millivolts	e_r volts	i milliamps	P milliwatts	ΔW millijoules
Armature open -					
0	234	29.0	0	0	-
1.0	204	25.5	22.88	583.5	.292
2.0	176	22.0	38.72	851.8	.718
3.0	150	18.8	51.48	967.8	.904
4.0	130	16.3	62.48	1018.4	.987
4.5	122	15.3	68.2	1043.5	.516
5.0	178	22.3	69.52	1550.3	.649
Armature closed					
6.3	-	*38.3	57.2	2190.8	2.433
6.5	174	15.4	58.08	894.5	.309
7.5	114	10.1	71.28	719.9	.808
9.0	74	6.6	87.56	578.0	.977
10.0	54	4.8	95.48	458.0	.518
11.0	36	3.2	101.2	324.0	.391
12.0	28	2.5	106.48	266.0	.295
13.5	18	1.6	112.2	180.0	.334
16.0	11	1.0	117.48	117.0	.374
18.5	5	0.5	119.68	60.0	.228
21.0	0	0	120.56	0	.075

Total Inductive Energy Input = 10.83

*This value was estimated since e_s was off scale

Legend: e_s - Search Coil Voltage
 e_r - Relay Coil Induced Voltage
 i - Relay Coil Current
P - Inductive Power
W - Inductive Energy

The power vs time relationship of Table I is plotted in Figure 19. As shown by Table I, the calculated $e_r = 29$ volts at $t = 0$. In the circuit equation

$$e = iR + N \frac{d\phi}{dt}$$

$e_r = N d\phi/dt$. Since $iR = 0$ at $t = 0$, e_r would be equal to the applied potential of 28 volts. The calculated e_r is very close to the actual value considering the large number of measurements involved.

The data from Figure 8 are listed in Table II.

TABLE II

INDUCTIVE ENERGY DISSIPATED DURING RELEASE CYCLE

Time millisec	e_s millivolts	e_r volts	i milliamps	P milliwatts	ΔW millijoules
Armature closed -					
0	940	82.7	126.0	10420	-
0.6	540	47.5	41.8	1985	3.72
2.0	300	26.4	22.0	581	1.8
4.4	120	10.6	8.3	88	0.74
Armature open -					
5.0	140	17.5	8.3	145	0.07
8.0	40	5.0	2.2	11	0.23
16.0	0	0	0	0	0.05
Total Energy Dissipated =					6.41

Legend: Same as Table I

As shown in Table II, the total energy dissipated during the release cycle is considerably less than the total input during the closing cycle as shown in Table I. Part of this difference is due to the energy delivered during the closing cycle to the mechanical system to overcome the friction and spring tension in closing the armature. The energy input during the period of armature motion is shown by the shaded area of Figure 19. This area represents about 3 millijoules of energy. Subtracting this amount from the total input leaves approximately 7.8 millijoules.

Another source of error in the energy calculation of Table II is

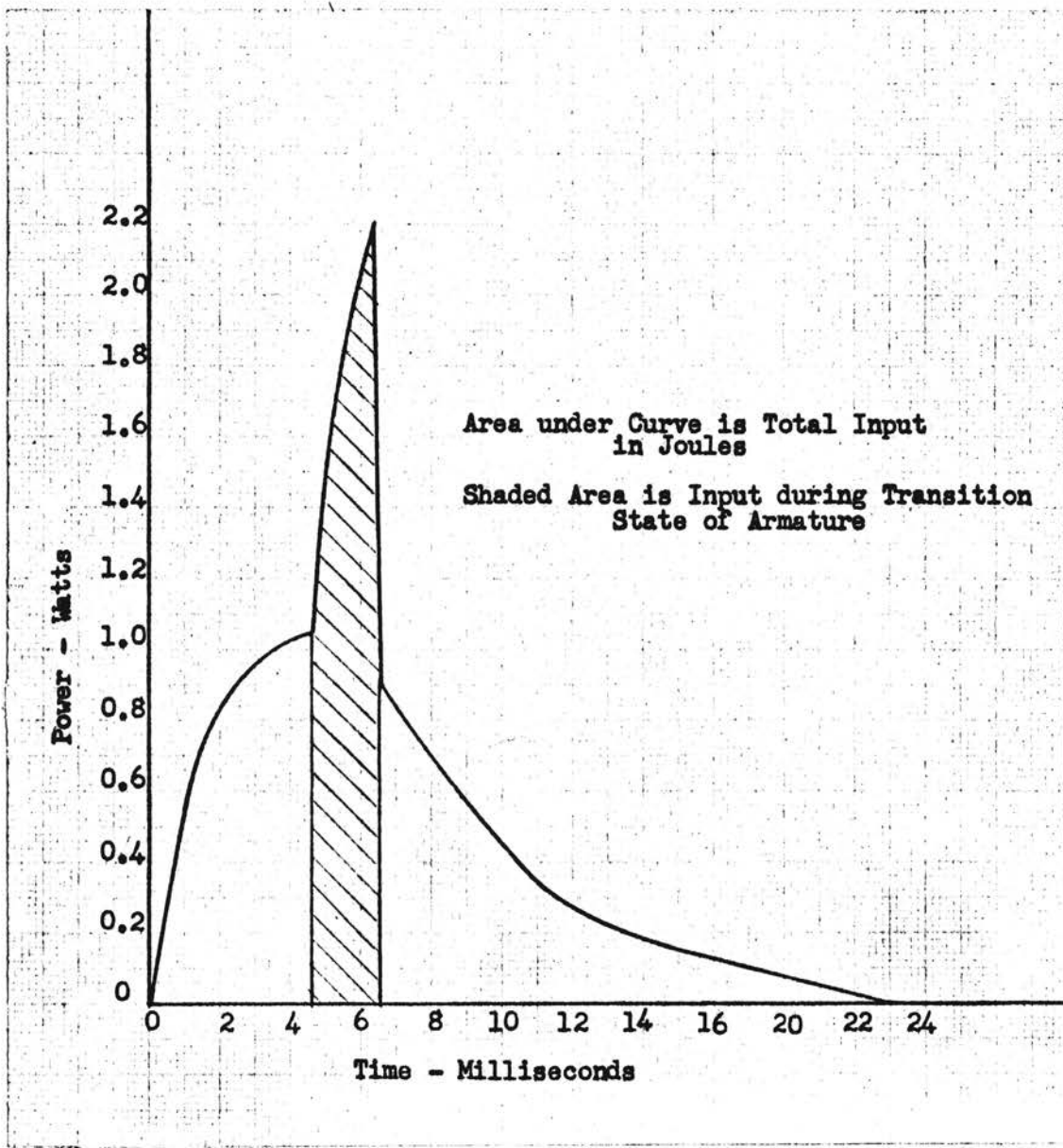


FIGURE 19 - INDUCTIVE ENERGY INPUT DURING CLOSING CYCLE

the time lag of the oscilloscope trace of the search coil voltage at time zero. Since the induced emf, e_r , was discharging into a total resistance of 1220 ohms, (relay coil, 220 ohms, plus discharge resistance, 1000 ohms), e_r should equal iR or $.126 \times 1220 = 154$ volts. A corrected W for the period 0 to 0.6 milliseconds based on this value of e_r at time zero would give 6.5 millijoules, thereby increasing the total energy dissipation some 2.78 millijoules. However, this value would not be exact either since the power relationship during the period 0 to 0.6 milliseconds does not have a constant slope but is actually a product of two functions approaching an exponential decay rate. Therefore, the energy dissipation for the period 0 to 0.6 milliseconds should be somewhere between 3.72 and 6.5 millijoules, and the total energy dissipation is probably very close to the figure of 7.8 joules. Therefore, it seems reasonable to assume that most of the energy input during the transition state is delivered to the mechanical system, and that the energy stored in the relay during the closing cycle was nearly equal to 7.8 joules.

The data from Figures 9 and 10 are listed in Tables III and IV, respectively. Some of the difference in the energy inputs with the

TABLE III

INDUCTIVE ENERGY INPUT WITH ARMATURE BLOCKED OPEN

Time millisec	e_s millivolts	e_r volts	i milliamps	P milliwatts	ΔW millijoules
0	240	30.0	0	0	-
2	175	21.8	32.3	705	0.70
4	128	16.0	57.5	920	1.63
6	92	11.5	76.3	876	1.80
8	64	8.0	94.0	752	1.63
10	41	5.1	105.0	535	1.29
12	24	3.0	114.5	344	0.88
15	12	1.5	120.0	180	0.64
20	0	0	125.0	0	0.45
Legend: Same as Table I					Total Energy Input = 9.02

TABLE IV

INDUCTIVE ENERGY INPUT WITH ARMATURE BLOCKED CLOSED

Time millisec	e_s millivolts	e_r volts	i milliamps	P milliwatts	ΔW millijoules
0	346	30.0	0	0	-
3	290	25.6	24.3	622	0.94
6	128	11.3	69.0	772	2.09
8	60	5.3	94.6	502	1.27
11	25	2.2	115.0	232	1.10
15	6	0.5	123.0	62	0.59
20	0	0	125.0	0	0.15
Total Energy Input =					<u>6.14</u>

Legend: Same as Table I

armature blocked open and blocked closed is due to the larger average inductance of the circuit with the armature open. However, the total difference in the two figures is more than is normally expected even with the nonlinearities present. A careful check of the data of Tables III and IV did not reveal any appreciable error and the data of Table V are further evidence of the accuracy of Table IV. The larger differences in incremental energy input (ΔW) for the two armature conditions occur after 6 milliseconds, indicating that saturation has occurred rapidly during the blocked closed condition. This would perhaps result in a sufficient variation of inductance during the transient period to produce the observed results.

As expected, the total energy of 9.02 millijoules shown in Table III was more than the stored energy of 7.8 millijoules during the normal closing cycle since the armature was open throughout the complete transient period.

Table V shows the energy dissipated during the release cycle with the armature blocked closed (refer to Figure 11). The same type of error is present at time zero as that discussed on pp. 35 and 37 for the normal release cycle. However, the totals of Tables IV and V compare

more favorably so that the error apparently is smaller in this case.

TABLE V

INDUCTIVE ENERGY DISSIPATED WITH ARMATURE BLOCKED CLOSED

Time millisec	e_s millivolts	e_r volts	i milliamps	P milliwatts	ΔW millijoules
0	880	77.4	125	9680	-
0.5	520	45.8	50.5	2313	3.0
1.0	360	31.7	30.8	976	0.82
1.5	280	24.6	22.0	541	0.38
2.0	240	21.1	17.2	363	0.23
3.0	188	16.5	12.3	203	0.28
5.0	120	10.6	7.2	76	0.28
8.0	52	4.6	2.6	12	0.13
10.0	0	0	0	0	0.01
Total Energy Dissipated =					<u>5.13</u>

Legend: Same as Table I

Table VI shows the data of Figure 12. The applied voltage was

TABLE VI

INDUCTIVE ENERGY INPUT AT 7 VOLTS D-C

Time millisec	e_s millivolts	e_r volts	i milliamps	P milliwatts	ΔW millijoules
0	58	7.25	0	0	-
2	42	5.25	11.0	57.8	0.06
4	30	3.75	17.6	66.0	0.06
7	20	2.5	22.0	55.0	0.09
10	13.2	1.65	26.0	42.9	0.07
15	7.0	0.88	28.6	25.2	0.17
21	0	0	31.2	0	0.08
Total Energy Input =					<u>0.53</u>

Legend: Same as Table I

just below the level at which the armature starts to move. However, this data does not give the energy input during the open state of a normal closing cycle at 28 volts d-c, since the current levels are not equal. The current data of Table VI will be used to determine the relay inductance during the open state.

Table VII shows the data as the applied relay voltage is increased

TABLE VII

INDUCTIVE ENERGY INPUT AS APPLIED VOLTAGE IS
INCREASED FROM 8 TO 28 VOLTS D-C

Time millisec	e_s millivolts	e_r volts	i milliamps	P milliwatts	ΔW millijoules
0	192.0	16.9	*25.5	430.0	-
2	88.5	7.8	67.3	525.0	0.96
4	43.0	3.8	91.5	348.0	0.87
6	20.0	1.8	104.5	189.0	0.54
8	10.0	0.9	112.5	126.0	0.32
10	5.0	0.4	116.5	47.0	0.17
15	0	0	120.0	0	0.12
Total Energy Input =					2.98

Legend: Same as Table I

*25.5 milliamps initial current due to 8 volt bias

from 8 to 28 volts d-c by a step function (Figure 13). The armature is closed in this case, and these measurements were taken to determine the relay inductance with the armature closed. The data of Figures 12 and 13 are being studied in an effort to find a more accurate method of determining the relay inductance.

The sum of the totals of Tables VI and VII are not the same as the energy stored during the closing cycle at 28 volts since the current levels do not correspond to the open and closed states of the armature.

INDUCTIVE ENERGY CALCULATIONS USING ONLY COIL CURRENT DATA

This method is exact for a circuit containing only linear inductance. The coil current data are easy to obtain, even on hermetically sealed relays, and it is desirable to use this method when it is sufficiently accurate. However, since there are known to be some nonlinearities in the inductance of relay circuits, it is necessary to compare this method with a method of known accuracy.

To demonstrate the degree of nonlinearity present at various conditions, the current data of Figures 7 through 13 were plotted on semi-log paper in Figures 20 through 23. A linear inductive current would be a straight line on this type of plot.

Since the inductance of the relay varies with time during the transient period, the inductance was calculated from coil current data for small periods of time (Δt). The derivation of the method used to calculate $L(\Delta t)$ is present in the appendix.

The inductive energy was calculated by the relationship

$$W_L \text{ (joules)} = \frac{L \text{ (henries)} \times [I \text{ (amps)}]^2}{2}.$$

However, since the total transient period was divided into several Δt 's, it was necessary to modify the formula as

$$W_L = \sum_1^n \left[\frac{L \times (I_2^2 - I_1^2)}{2} \right] \Delta t_n$$

where I_2 and I_1 are final and initial values of current during the period Δt and L is the inductance during the corresponding period.

The current during the closing cycle of Figure 7 is plotted in Figure 20. The values of inductance during the various Δt 's are tabulated in Table VIII. The energy inputs for various Δt 's are also tabulated and the totals calculated. A set of sample calculations is shown below for line 3 of Table VIII.

Sample Calculations

Data from line 3, Table VIII

Time = 2 milliseconds, $i = 39$ milliamps

$i'(t) = I(\text{steady state}) - i(t) = 122 - 39 = 83$ milliamps

Note: In order to observe nonlinearity of inductance on a semi-log plot, it is necessary to plot $i'(t)$ rather than $i(t)$.

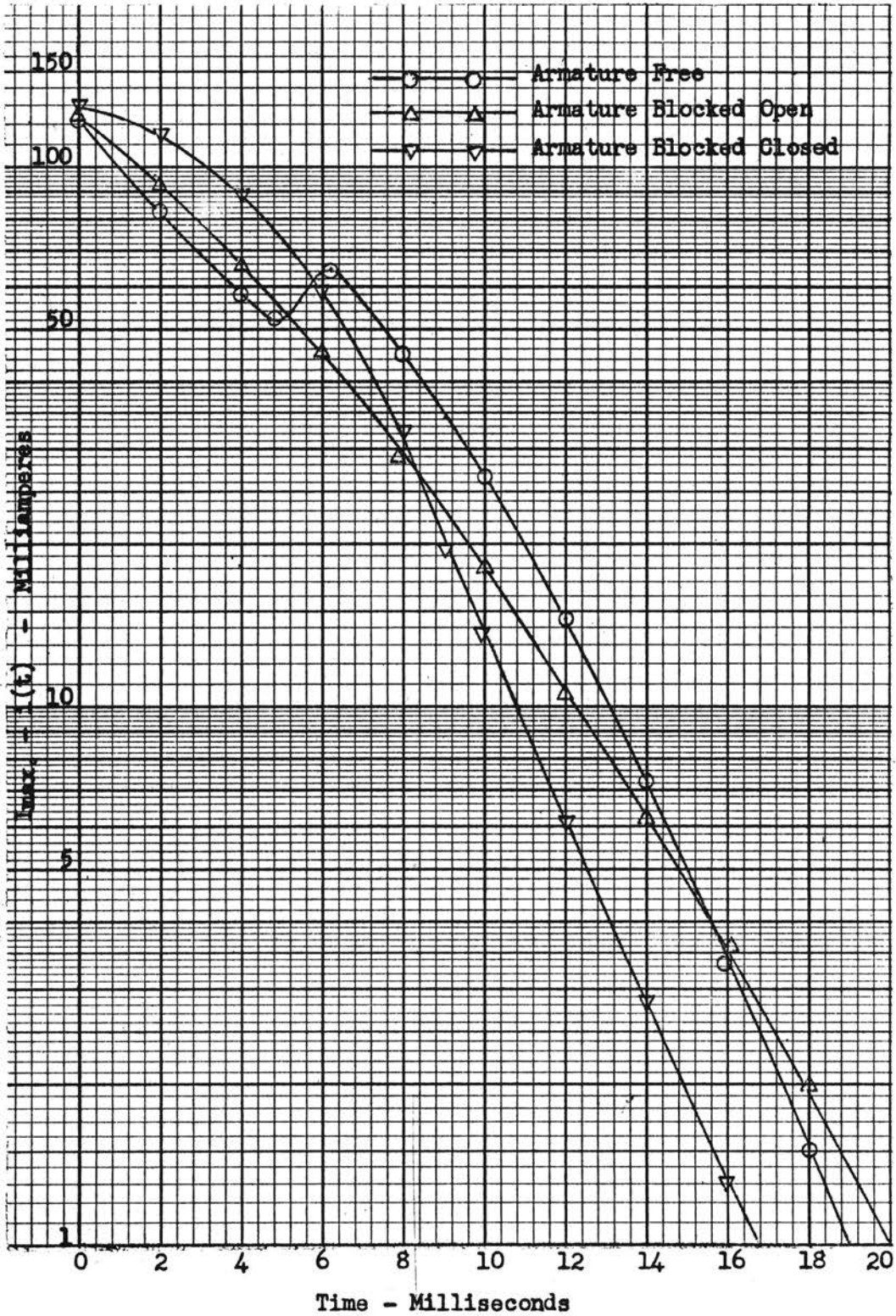


FIGURE 20 - RELAY COIL CURRENT BUILDUP AT 28 VOLTS D-C

$$\text{Slope} = \frac{\ln I_1' - \ln I_2'}{t} = \frac{\ln .099 - \ln .083}{.002 - .001} = \frac{-2.31 - (-2.49)}{.001} = 180$$

$$L(\Delta t) = \frac{R}{\text{Slope}} \times 10^3 = \frac{230}{180} \times 10^3 = 1278 \text{ millihenries, where } R =$$

resistance of relay coil plus series resistance.

$$W = \frac{L(I_2'^2 - I_1'^2)}{2} = \frac{1278 (.039^2 - .023^2)}{2} = 0.63 \text{ millijoules}$$

The average inductance is calculated by

$$L_{\text{ave}} = \sum \frac{L(\Delta t) \times \Delta t}{T}$$

where T is the total transient period. The effective inductance is determined by

$$L_{\text{eff}} = R \times T'$$

where T' is the time at which the current is equal to 63.2% of the steady state value.

TABLE VIII

INDUCTIVE ENERGY INPUT DURING CLOSING CYCLE

Time millisec	i milliamps	i milliamps	ln i'	Slope	L(Δt) milli- henries	ΔW milli- joules
Armature open						
0	0	122	-2.1	-	-	-
1	23	99	-2.31	210	1095	0.29
2	39	83	-2.49	180	1278	0.63
3	53	69	-2.67	180	1278	0.83
4	64	58	-2.84	170	1353	0.87
4.5	68	54	-2.92	160	1438	0.36
Armature closed						
7	66	56	-2.88	-	-	-
9	87	35	-3.35	235	980	1.57
11	102	20	-3.91	280	820	1.15
13	111.5	10.5	-4.59	340	675	0.68
15	117	5.1	-5.29	350	657	0.43
17	119.6	2.35	-6.06	385	597	0.18
19	121	1.0	-6.9	420	548	0.16

Total Energy Input = 7.28

Legend: i - relay coil current

i' - steady state current minus i

L(Δt) - inductance during period Δt

W - inductive energy

In Table VIII, the inductive energy input was calculated only during the open and closed states of the armature, since the inductance during the transition state is difficult to determine. The values of average and effective inductance were both 715 millihenries during the closed state, and were also very close during the open state in spite of the large variations of inductance during the transient period. The average inductance during the open state was 1272 millihenries compared to an effective inductance of 1222 millihenries.

The inductive energy dissipated during the release cycle is tabulated in Table IX. As in the case of Table VIII, the energy is determined only

TABLE IX

INDUCTIVE ENERGY DISSIPATED DURING RELEASE CYCLE

Time millisec	i milliamps	*ln i	Slope	L(Δt) millihenries	ΔW millijoules
Armature closed					
0	126	-2.07	-	-	-
0.6	41.8	-3.17	1833	674	4.75
2.0	22.0	-3.82	457	2691	1.74
4.4	8.3	-4.69	362	3397	0.7
Armature open					
5.0	8.3	-4.69	-	-	-
8.0	2.2	-6.12	476	2584	0.08
10.0	1.0	-6.91	395	3114	0.01
16.0	0	-	-	-	0
Total Energy Dissipated =					<u>7.28</u>

*In the case of decreasing current, it is not necessary to plot i'

L_{ave} = 2750 millihenries during closed state
 = 2796 during open state
 L_{eff} = 550 millihenries during closed state
 = 1900 during open state

Legend: i - instantaneous coil current
 L(Δt) - inductance during period Δt
 W - inductive energy dissipated

during the open and closed states of the armature and the totals of Tables VIII and IX are exactly equal. The values of average and effective inductance are vastly different in this case. The extreme variations of

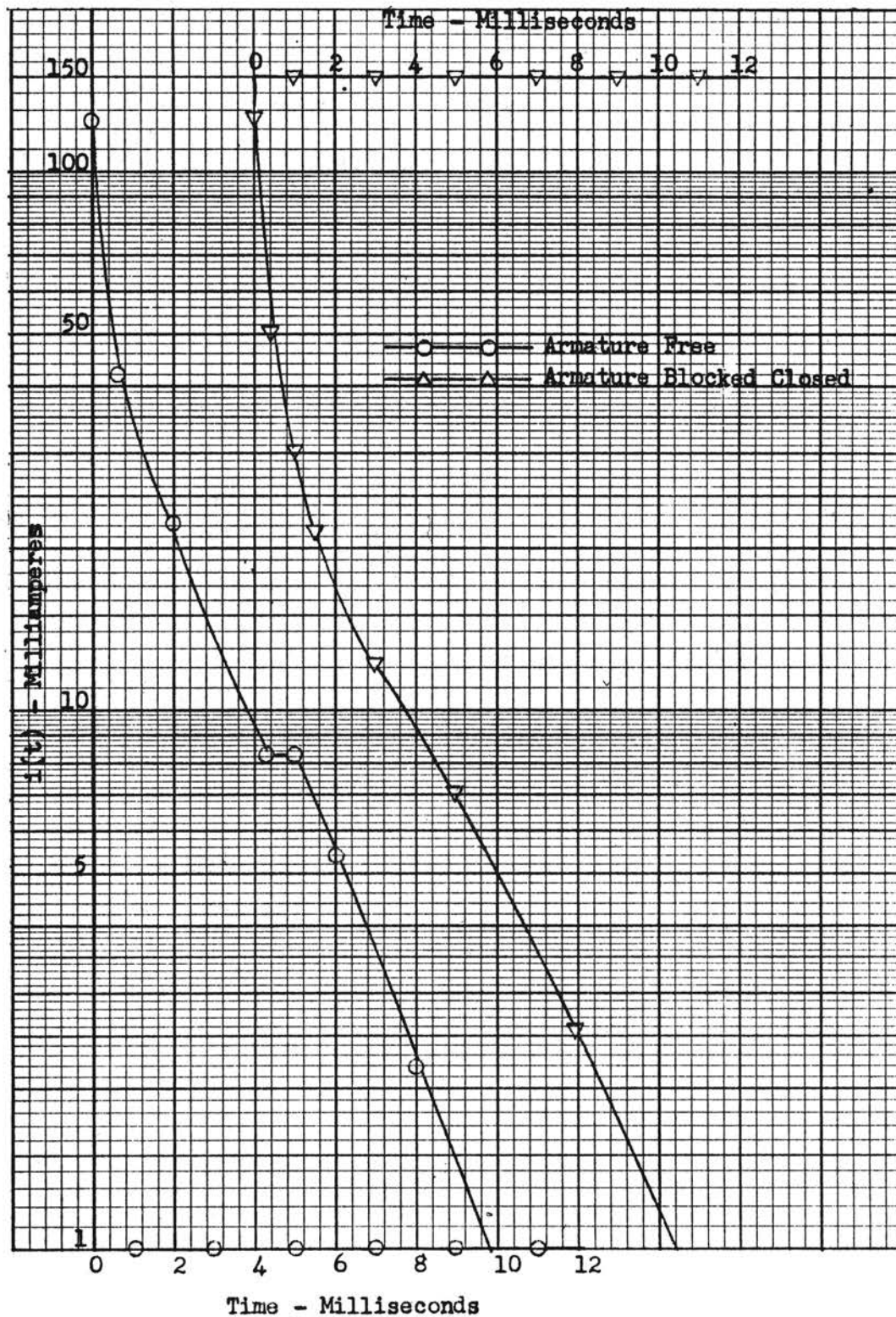


FIGURE 21 - RELAY COIL CURRENT DECAY AT 28 VOLTS D-C

inductance during the transient period are illustrated by the large changes of slope of the current vs time curve of Figure 21.

The inductive energy input with the armature blocked open is shown in Table X. As expected the energy input is slightly higher than that shown in Table VIII since the open armature inductance is present throughout the transient period. The inductance values compare favorably with

TABLE X

INDUCTIVE ENERGY INPUT WITH ARMATURE BLOCKED OPEN

Time millisec	i milliamps	i milliamps	$\ln i'$	Slope	L(Δt) milli- henries	ΔW milli- joules
0	0	126.0	-2.07	-	-	-
2	33.3	92.7	-2.38	155	1420	0.8
4	59.0	67.0	-2.7	160	1375	1.63
6	79.3	46.7	-3.06	180	1222	1.72
8	95.0	31.0	-3.47	205	1073	1.47
10	106.0	20.0	-3.91	220	1000	1.11
12	114.5	11.5	-4.46	255	863	0.81
15	120.2	5.8	-5.15	230	957	0.64
20	125.0	1.0	-6.91	253	870	0.62
Total Energy Input =						8.8

$L_{ave} = 1056$ millihenries

$L_{eff} = 1270$ millihenries

Legend: Same as Table VIII

those for the corresponding times of the open armature period during the normal closing cycle.

The data of Tables XI and XII give a comparison of the energy relationships with the armature blocked closed. Both the energy stored (Table XI) and the energy dissipated (Table XII) were somewhat higher than expected. Actually the two values should have been equal. Errors are thereby indicated in these values. The assumption of error is supported by comparison of the total of Table XI with the energy stored during the closing cycle (Table VIII). The two figures are almost equal whereas the value of Table XI should have been less since the armature

was closed during the entire transient period.

TABLE XI

INDUCTIVE ENERGY INPUT WITH ARMATURE BLOCKED CLOSED

Time millisec	i milliamps	i' milliamps	ln i'	Slope	L(Δt) milli- henries	ΔW milli- joules
0	0	126.0	-2.07	-	-	-
3	23.1	102.9	-2.37	100	2200	0.58
6	66.0	60.0	-2.81	147	1507	2.85
8	93.7	32.3	-3.43	310	710	1.58
11	116.0	10.0	-4.5	357	616	1.35
15	124.0	2.0	-5.81	327	673	0.64
20	126.0	0.7	-7.41	320	688	0.25
Total Energy Input =						<u>7.25</u>

$L_{ave} = 1026$ millihenries

$L_{eff} = 1400$ millihenries

Legend: Same as Table VIII

TABLE XII

INDUCTIVE ENERGY DISSIPATED WITH ARMATURE BLOCKED CLOSED

Time millisec	i milliamps	ln i	Slope	L(Δt) millihenries	ΔW millijoules
0	125	-2.07	-	-	-
0.5	50.5	-2.9	1660	735	4.81
1.0	30.8	-3.48	1160	1052	0.84
1.5	22.0	-3.82	680	1794	0.42
2.0	17.2	-4.06	480	2541	0.23
3.0	12.3	-4.38	320	3813	0.28
5.0	7.2	-4.93	275	4436	0.22
8.0	2.6	-5.96	343	3557	0.09
10.0	0	-	-	-	0
Total Energy Dissipated =					<u>6.89</u>

Discharge R = 1230 ohms

$L_{ave} = 2641$ millihenries

$L_{eff} = 684$ millihenries

Legend: Same as Table IX

The current vs time data of Figures 22 and 23 were used to calculate the data of Tables XIII and XIV, respectively. The energy values in these tables have no significance except for these particular conditions and

do not represent energy storage during the open and closed states. The energy values were calculated in order to compare with those of Table VI and VII. These conditions were actually studied in an effort to arrive at a more accurate method of determining the relay inductance during the open and closed states.

TABLE XIII

INDUCTIVE ENERGY INPUT AT 7 VOLTS D-C

Time millisec	i milliamps	i' milliamps	ln i'	Slope	L(Δt) milli- henries	ΔW milli- joules
0	0	31.2	-3.47	-	-	-
2	11.0	20.2	-3.9	215	1045	0.063
4	17.6	13.6	-4.31	205	1097	0.098
7	22.7	8.5	-4.77	153	1468	0.143
10	25.8	5.4	-5.22	150	1500	0.12
15	28.6	2.6	-5.96	148	1520	0.12
21	31.2	0	-	-	1520	0.12
Total Energy Input =						<u>0.664</u>

$$L_{ave} = 1420 \text{ millihenries}$$

$$L_{eff} = 1150 \text{ millihenries}$$

Legend: Same as Table VIII

TABLE XIV

INDUCTIVE ENERGY INPUT AS VOLTAGE IS INCREASED
FROM 8 TO 28 VOLTS D-C

Time millisec	i milliamps	i' milliamps	ln i'	Slope	l(Δt) milli- henries	ΔW milli- joules
0	25.5	94.5	-2.36	-	-	-
2	67.3	52.7	-2.94	290	790	1.09
4	91.5	28.5	-3.56	310	740	1.42
6	104.5	15.5	-4.17	305	755	0.96
8	112.5	7.5	-4.89	360	640	0.68
10	116.5	3.5	-5.65	380	605	0.25
13	120.0	0	-	-	605	0.25
Total Energy Input =						<u>4.65</u>

$$L_{ave} = 680 \text{ millihenries}$$

$$L_{eff} = 740 \text{ millihenries}$$

Legend: Same as Table VIII

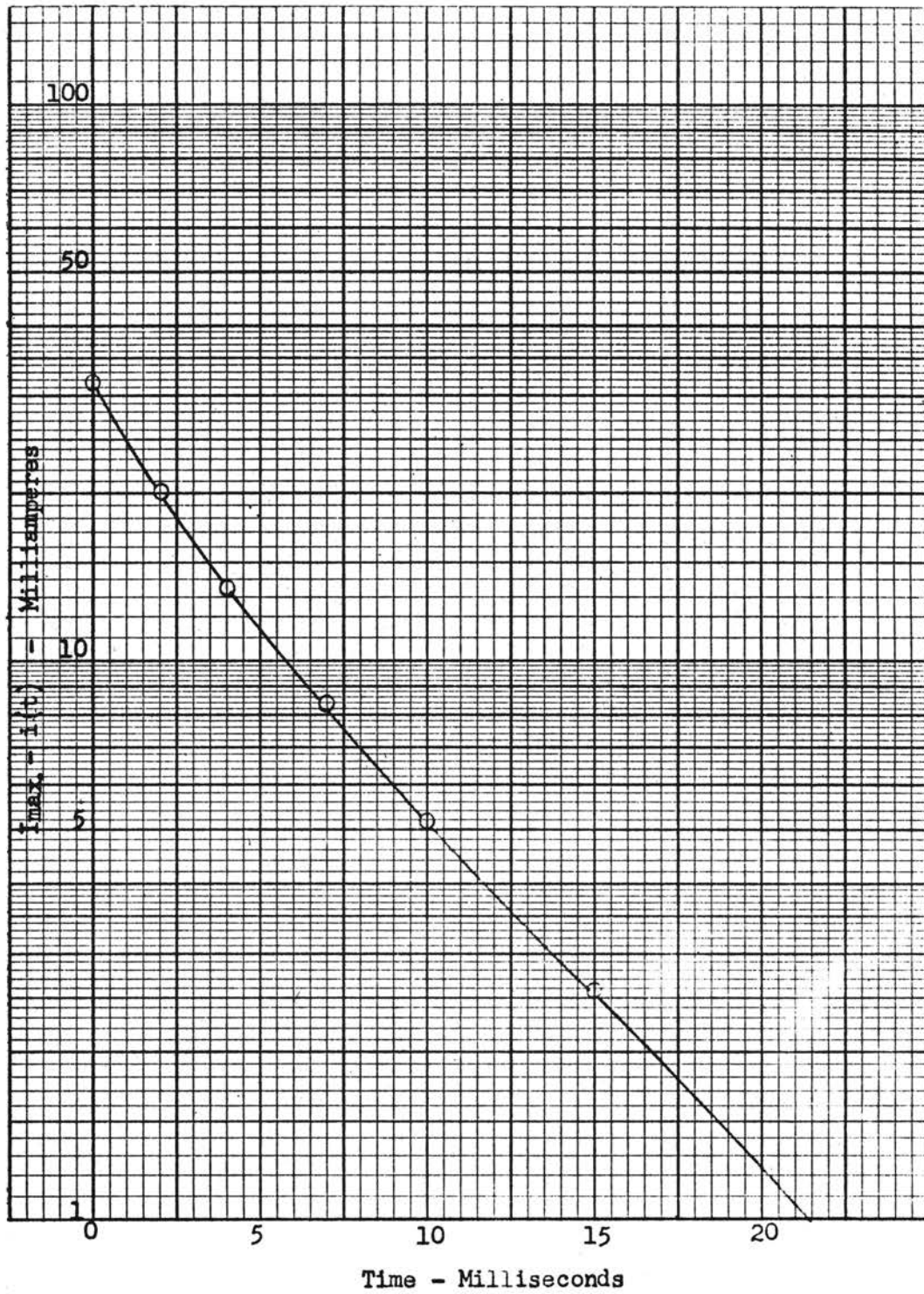


FIGURE 22 - RELAY COIL CURRENT BUILDUP AT 7 VOLTS D-C

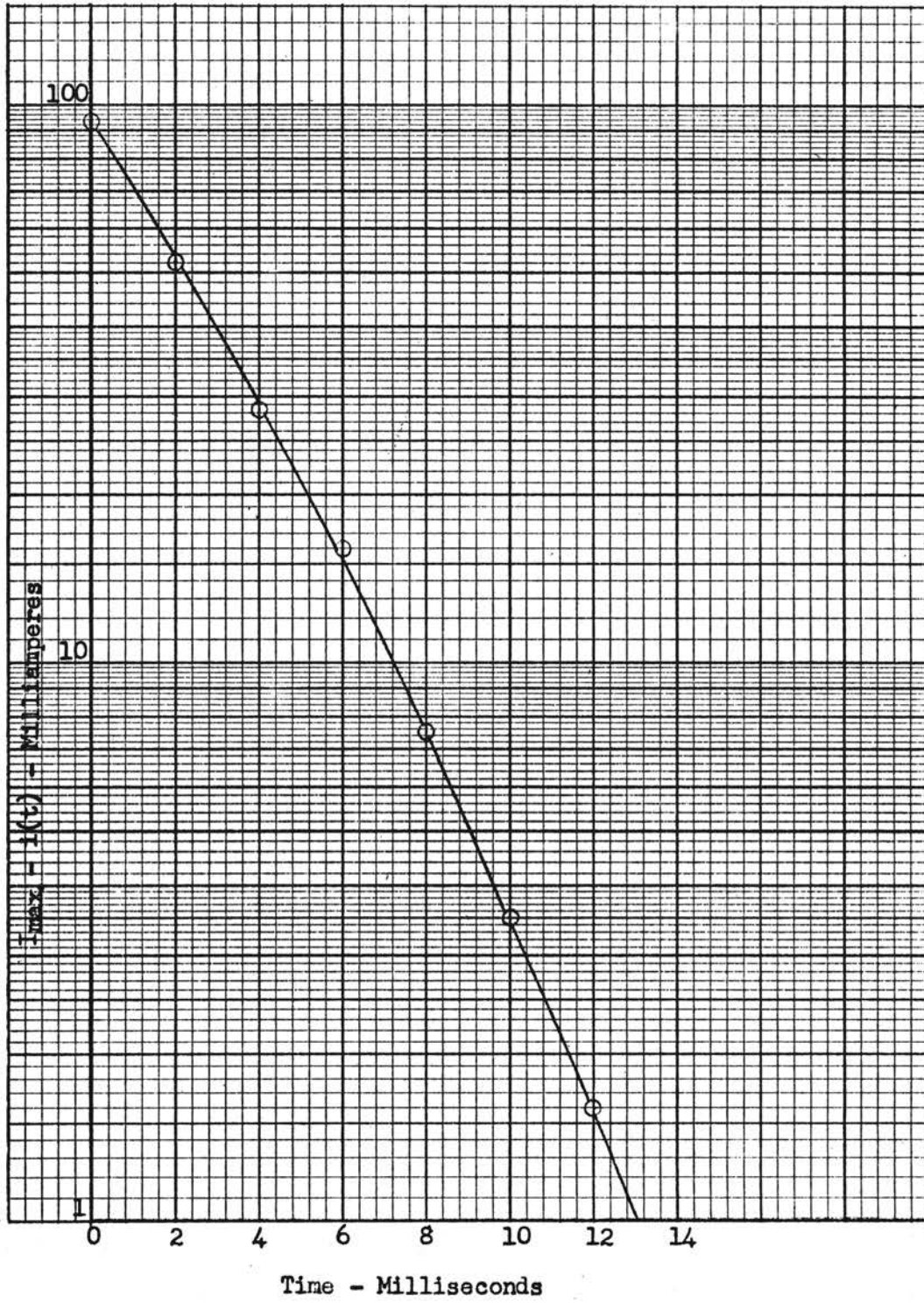


FIGURE 23 - RELAY COIL CURRENT BUILDUP WITH STEP INCREASE FROM 8 TO 28 VOLTS D-C

Comparison with Table VIII shows that the open and closed state inductances as determined by the latter two procedures do not differ greatly from those determined from data taken during the normal closing cycle. This indicates that the values of Table VIII are sufficiently accurate for most practical applications. It is somewhat doubtful that the procedure of Table XIV results in a significant improvement in accuracy, since the current levels are different than during the normal closing cycle. With the armature closed, the effect of the current level on saturation may offset the advantage of an expanded time scale. The difference in current levels has little effect on the saturation of the circuit with the armature open, and it is believed that the procedure of Table XIII will be more accurate in this case.

COMPARISON OF INDUCTIVE ENERGY RELATIONSHIPS AS DETERMINED BY FOUR METHODS

In this section the calculations of inductive energy by several different methods are tabulated and compared. For convenience the various methods are listed and discussed below:

Method number 1 - The data derived by this method are listed in Tables I through VII. This method employed the relationship $W_L = \int P dt$ modified to give $W_L = \sum P_{ave} \times \Delta t$ as discussed on p. 33. This is believed to be the most accurate method of determining inductive energy from measurements and will be used as a standard to determine the accuracy of the other methods.

Method number 2 - The data derived by this method are shown in Tables VIII through XIV. This method employed the relationship $W_L = LI^2/2$ modified to give $W_L = \sum L(I_2^2 - I_1^2)/2$ as discussed on p. 41. This has an advantage over Method 1 in that only the relay coil current

measurements are needed.

Method number 3 - This method employs the relationship $W_L = LI^2/2$ and consists of a single calculation for the entire transient period with L equal to the average inductance during the period. The values of L_{ave} used for these calculations were determined from Tables VIII through XIV. This method would not be exact except for linear inductance but involves much less time and rigor than Method 1 and 2 and would be useful if sufficiently accurate.

Method number 4 - This is the same as Method 3 except that L_{ave} as determined in Tables XIII and XIV are used in lieu of the L_{ave} calculated from the actual measurements. As discussed on p. 48 the data of Tables XIII and XIV were taken in an attempt to find more accurate methods of determining the relay inductance during the open and closed states. If the inductance values thus determined are realistic, Method 4 should provide energy values of fairly good accuracy and would be a relatively simple method of calculation.

The effective inductances listed in Tables VIII through XIV are not used to calculate energy relations since they do not show a consistent pattern of accuracy.

The results of all calculations are shown in Table XV. Very good accuracy for Method 2 is indicated for all conditions except 5 and 7. The large errors of this method during these conditions are hard to explain. There are some rather large variations of inductance during these conditions because of the armature being in the closed position throughout the entire transient period. It is possible that the time increments used to calculate energy during these conditions were too large to give a high degree of accuracy. However, the results of Conditions 4 and 5, even with relatively large errors, are still usable with safety factors

within the range of good design practice.

TABLE XV
COMPARISON OF INDUCTIVE ENERGY AS DETERMINED
BY FOUR DIFFERENT METHODS

Condition	Method 1		Method 2		Method 3		Method 4	
	Energy	Error %	Energy	Error %	Energy	Error %	Energy	Error %
1	*7.8	0	7.28	-6.7	**6.46	-17.2	6.77	-13.2
2	6.4	0	7.28	+13.7	**20.3	+217.0	-	-
3	9.02	0	8.8	-2.4	8.34	-7.5	10.20	+13.1
4	6.14	0	7.25	+18.0	8.1	+31.9	5.37	-12.5
5	5.13	0	6.89	+34.0	20.9	+308.0	-	-
6	0.53	0	0.66	+24.5	0.69	+30.2	-	-
7	2.98	0	4.65	+56.0	5.03	+69.0	-	-

Energy in millijoules

- Condition 1 - Normal closing cycle, 28 volts d-c, energy stored
 Condition 2 - Normal release cycle, 28 volts d-c, energy dissipated
 Condition 3 - Armature blocked open, 28 volts d-c, energy input
 Condition 4 - Armature blocked closed, 28 volts d-c, energy input
 Condition 5 - Armature blocked closed, 28 volts d-c, energy dissipated
 Condition 6 - Armature open, 8 volts d-c, energy input
 Condition 7 - Armature closed, increase from 8 to 28 volts d-c, energy input

*Estimated by subtracting input during transition state from the total input.

**Calculated using L_{ave} 's during both open and closed states.

There is some doubt about the accuracy of Method 1 for a decaying energy cycle as discussed on p. 37. Since the energy dissipated is believed to be more than actually shown by Method 1, the error of Method 2 for Condition 5 may be somewhat exaggerated. This is also true for Condition 2.

Method 3 appears to be reasonable accurate except for Conditions 2 and 5 when the release cycle was involved. It is obvious that an accurate calculation of average inductance is difficult when there are large variations in the rate of change of current as shown in Figures 8 and 10. Therefore, the concept of average inductance does not seem to

be very useful in these cases.

The application of Method 4 in lieu of Method 3 reduced the error in each case. This attests to the advantage of measuring the inductance by Procedures 6 and 7. Method 4 is apparently a reasonably accurate method and also requires very little time and rigor as compared to Methods 1 and 2.

The results of Method 2 for conditions 1, 2 and 3 are close enough to Method 1 data that the differences can be chiefly attributed to instrumentation and operator errors incurred while making the measurements.

INDUCTANCE STUDIES ON THREE ALLIED MHJ-18D RELAYS USING COIL CURRENT MEASUREMENTS

The data of Figures 14 through 18 were used to determine the inductances of three relays under identical conditions. Allied MHJ-18D relays, the same type used for the inductive energy studies, were used in this investigation. Since the purpose of this exercise was to compare the inductances of specimens of the same type, the inductive energy was not calculated. It was felt that the range of variation among the inductances of relays of the same type should be investigated, since this is one of the factors influencing the inductive energy storage.

The method discussed on p. 41 and p. 43 was used to determine the inductance during small increments of time (Δt). The average and effective inductance during the transient period were also calculated. Procedures 8 through 12, discussed on pp. 27-30, were followed in making the measurements. The current vs time characteristics were plotted in Figures 24 through 28.

Table XVI shows a compilation of the data for the normal closing

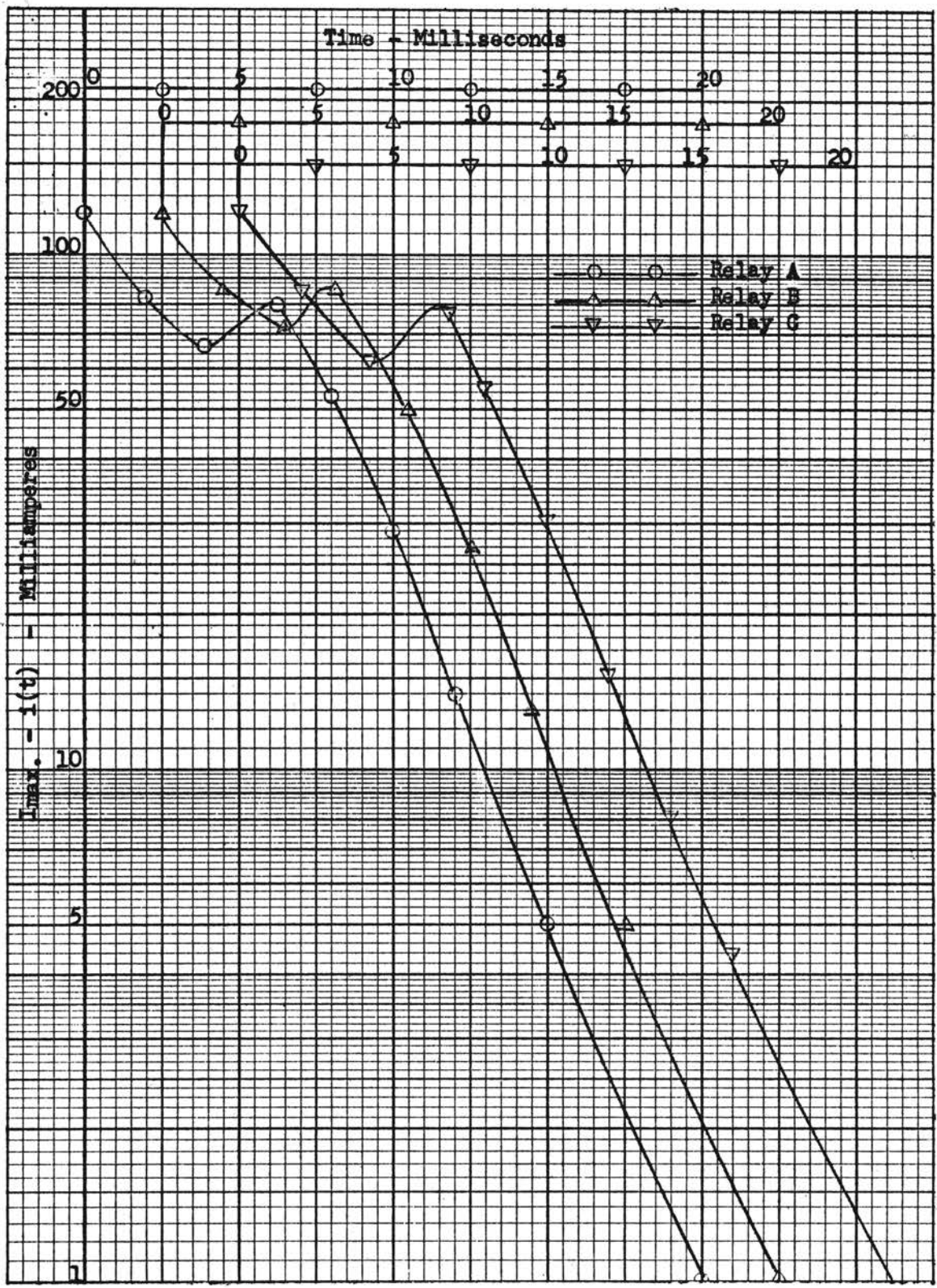


FIGURE 24 - RELAY COIL CURRENT BUILDUP AT 28 VOLTS D-C

TABLE XVI

INDUCTANCE OF RELAYS DURING NORMAL CLOSING CYCLE

Relay	Time milli- seconds	i milli- amps	i milli- amps	ln i'	Slope	R ohms	L(Δt) milli- henries	L _{ave} milli- henries	L _{eff} milli- henries			
A - armature open												
	0	0	124	-2.09	-	200	-	1350	1050			
	1	27	97	-2.34	250	↓	800	↓	↓			
	2	43	81	-2.51	170		1180					
	3	53	71	-2.65	140		1430					
	4	59	65	-2.75	100		2000					
armature closed												
	7	56	68	-2.69	-		-			634	670	
	9	84	40	-3.18	245		815			↓	↓	
	11	104	20	-3.91	365		550					
	13	114.5	9.5	-4.66	375		535					
	15	119	5.0	-5.3	320		625					
	17	121.4	2.7	-5.93	315	635						
	19	122.6	1.4	-6.55	310	645						
B - armature open												
	0	0	123	-2.1	-	200	-	1506	1090			
	1	22	101	-2.29	190	↓	1050	↓	↓			
	2	37	86	-2.46	170		1175					
	3	46	77	-2.57	110		1800					
	4	52	71	-2.67	100		2000					
armature closed												
	7	58	65	-2.73	-		-			617	677	
	9	85	38	-3.27	270		740			↓	↓	
	11	104	19	-3.96	345		580					
	13	114	9	-4.71	375		535					
	15	118.3	4.7	-5.36	325		615					
	17	120.5	2.5	-6.0	320	625						
	19	121.6	1.4	-6.66	330	605						

TABLE XVI - Continued

Relay	Time	i	i	$\ln i'$	Slope	R	$L(\Delta t)$	L_{ave}	L_{eff}	
C - armature open										
	0	0	122	-2.11	-	205 ↓	-	1335	1185	
	1	20	102	-2.28	170		1210	↓	↓	
	2	37	85	-2.46	180		1140	↓	↓	
	3	49	73	-2.62	160		1280	↓	↓	
	4	52	64	-2.74	120		1710	↓	↓	
armature closed										
	7	50	72	-2.63	-		-	667	695	
	9	70	42	-3.17	270		760	↓	↓	
	11	100.5	21.5	-3.85	340		600	↓	↓	
	13	111	11	-4.51	330		620	↓	↓	
	15	116	6	-5.12	305		660	↓	↓	
	17	118.8	3.3	-5.73	305		660	↓	↓	
	19	120.2	1.8	-6.31	290		705	↓	↓	

Legend: i - relay coil current
 i' - steady state current - i
 $L(\Delta t)$ - inductance during period Δt

cycle of Procedure 8, and is typical of the method used for all procedures. The inductances during the normal closing cycle are shown for both the open and closed states of the armature. Very good correlation between the relays is shown for average and effective inductance in both states.

The results of the studies under all conditions are summarized in Table XVII. The mean values of average and effective inductance were determined by adding the inductances of the three relays and dividing the total by three. The % deviation shown in the table are deviations from the mean.

Of the 18 individual inductance values (3 relays at 6 different conditions) the range of deviation is -11.6 to +14 percent. Actually, all values except the two extremes are within the range of -8.5 to +7.7 percent. This is strong evidence that inductance values do not vary greatly on relays of the same type and that measurements on a few relays of a given type will be sufficient to statistically predict the range of variation.

A comparison of Condition 3 with 4 and Condition 5 with 6 shows that the largest errors occur with the armature closed and with the largest voltage variation. This is as expected because of the greater effect of saturation under these conditions.

The effect of hysteresis on relay inductance is illustrated by comparison of Condition 3 with Condition 5. The inductance was less but the range of deviation was greater with decreasing voltage than with increasing voltage.

TABLE XVII

COMPARISON OF INDUCTANCES OF THREE ALLIED MHJ-18D RELAYS

Condition	Relay	L_{ave} mh	Deviation %	L_{eff} mh	Deviation %	Mean L_{ave} mh	Mean L_{eff} mh
1	A	1350	-3.8	1080	-3.4	1404	1118
	B	1506	+7.3	1090	-2.5		
	C	1355	-3.5	1185	+6.0		
2	A	634	-0.8	670	-1.0	639	677
	B	617	-3.5	667	-1.5		
	C	667	+4.4	695	+2.6		
3	A	600	+4.9	520	-0.1	572	522
	B	550	-3.8	500	-4.2		
	C	565	-1.2	545	+4.3		
4	A	495	-8.5	580	-2.1	537	592
	B	545	+1.5	580	-2.1		
	C	570	+6.1	615	+3.9		
5	A	470	-0.7	355	-2.1	473	363
	B	440	-7.1	355	-2.1		
	C	510	+7.7	380	+4.2		
6	A	970	+14.0	415	-6.0	854	442
	B	840	-1.9	465	+5.3		
	C	755	-11.6	445	+0.8		

Legend: mh - millihenries

Condition 1 - Normal closing cycle at 28 volts d-c,
armature open.

Condition 2 - Normal closing cycle at 28 volts d-c,
armature closed.

Condition 3 - Voltage increased from 17 to 28 volts d-c,
armature closed.

Condition 4 - Voltage increased from 12 to 28 volts d-c,
armature closed.

Condition 5 - Voltage decreased from 28 to 17 volts d-c,
armature closed.

Condition 6 - Voltage decreased from 28 to 7 volts d-c,
armature closed.

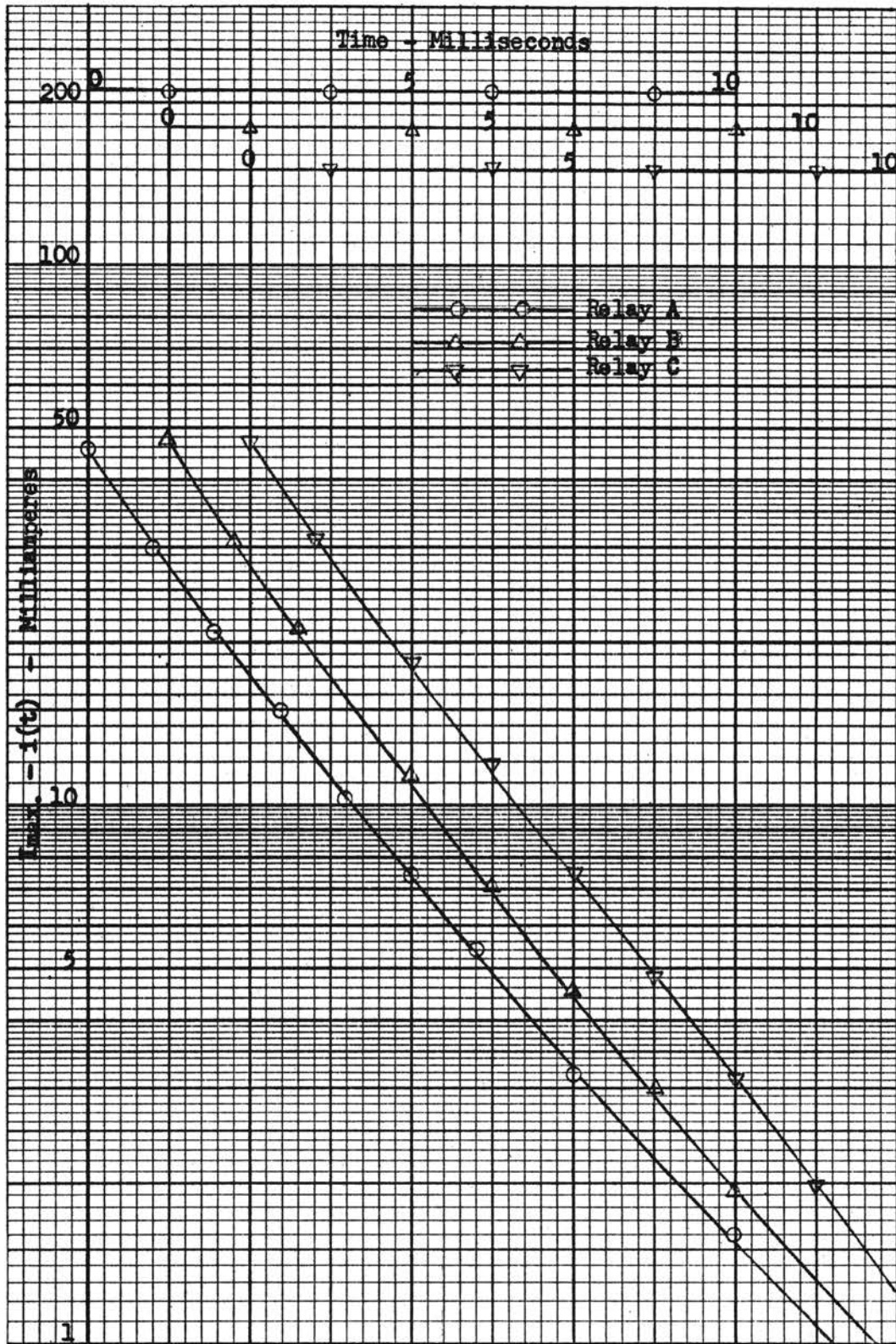


FIGURE 25 - RELAY COIL CURRENTS WITH STEP INCREASE FROM 17 TO 28 VOLTS D-C

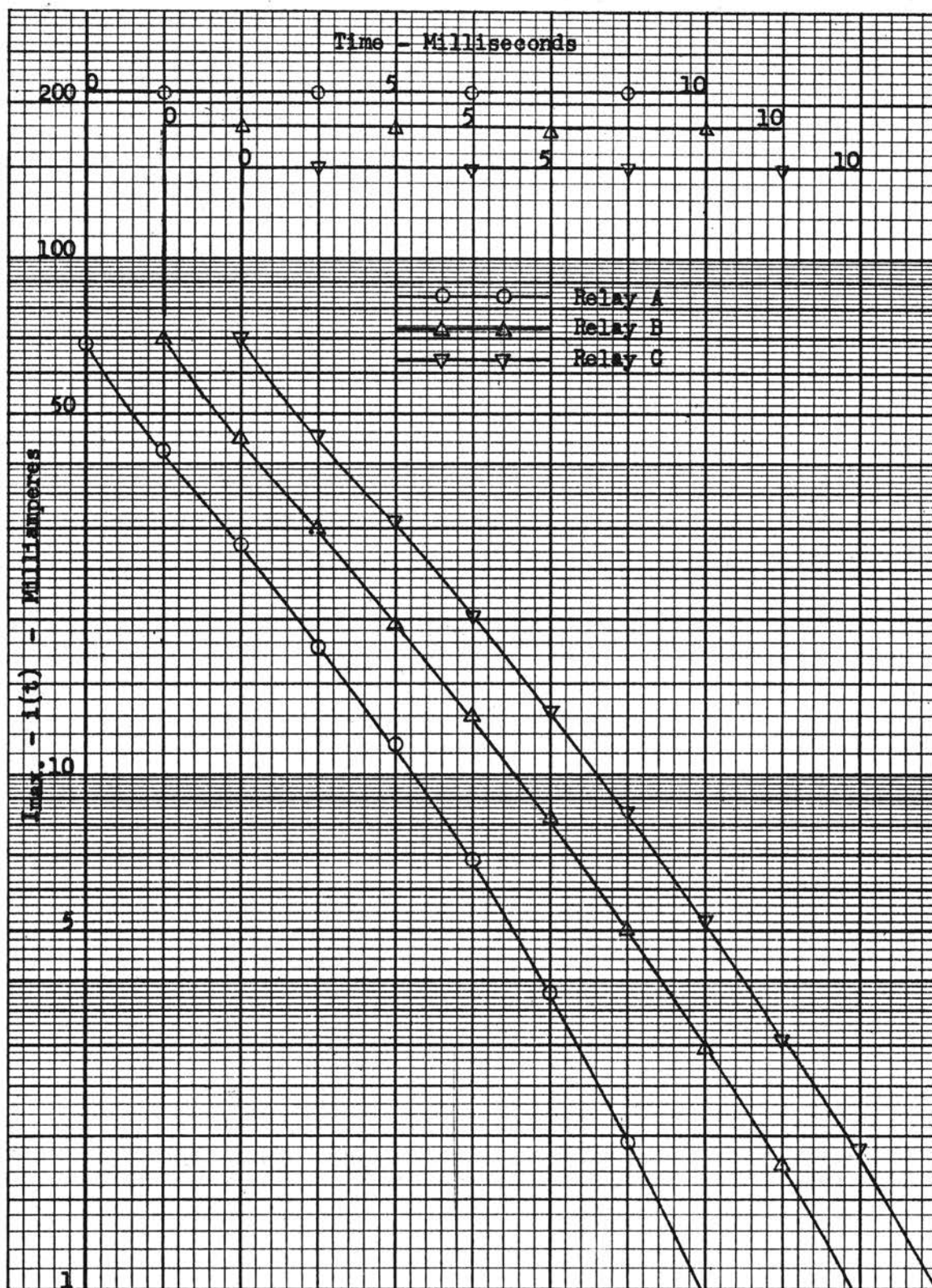


FIGURE 26 - RELAY COIL CURRENTS WITH STEP INCREASE FROM 12 TO 28 VOLTS D-C

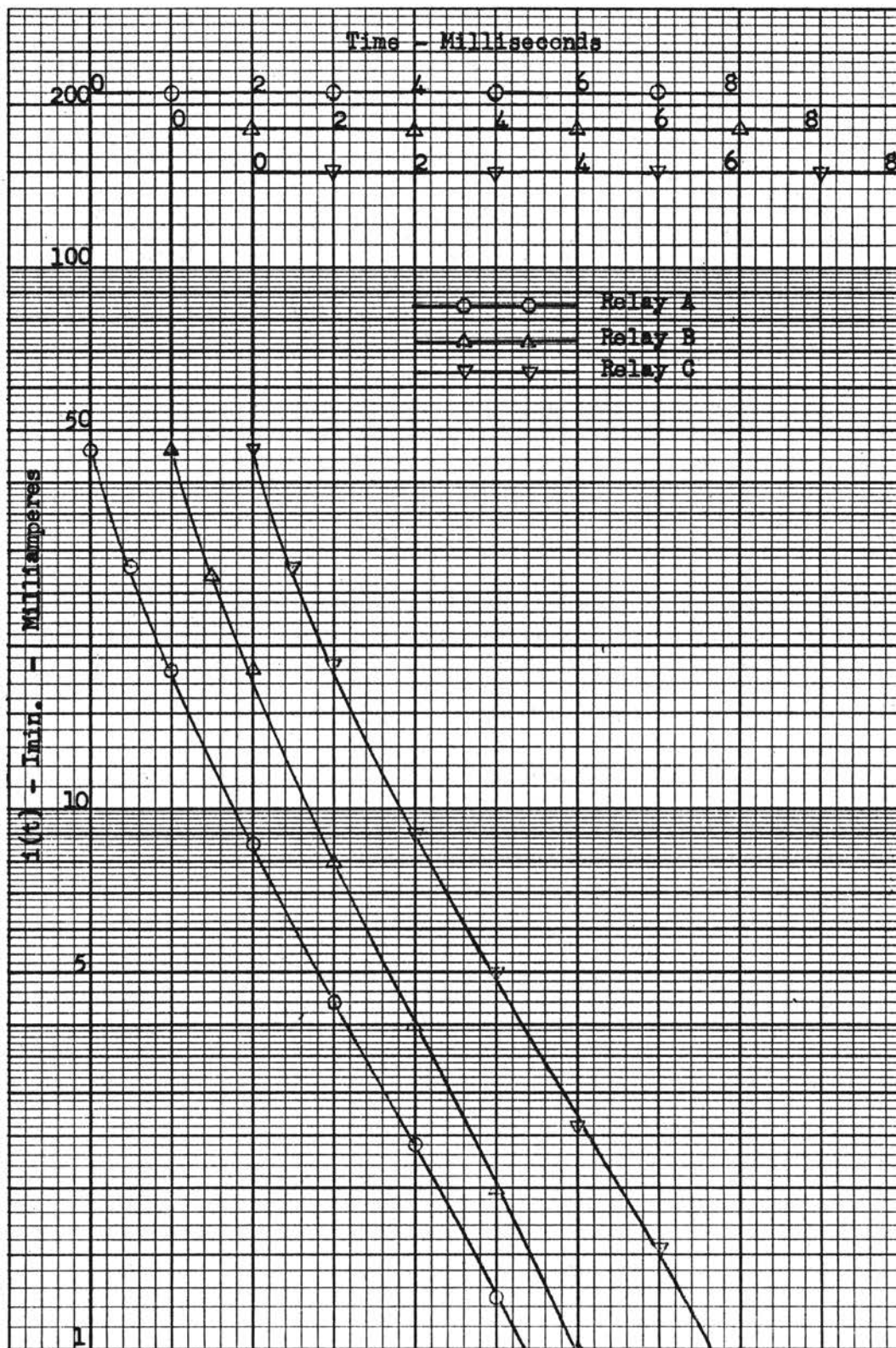


FIGURE 27 - RELAY COIL CURRENTS WITH STEP DECREASE FROM 28 TO 17 VOLTS D-C

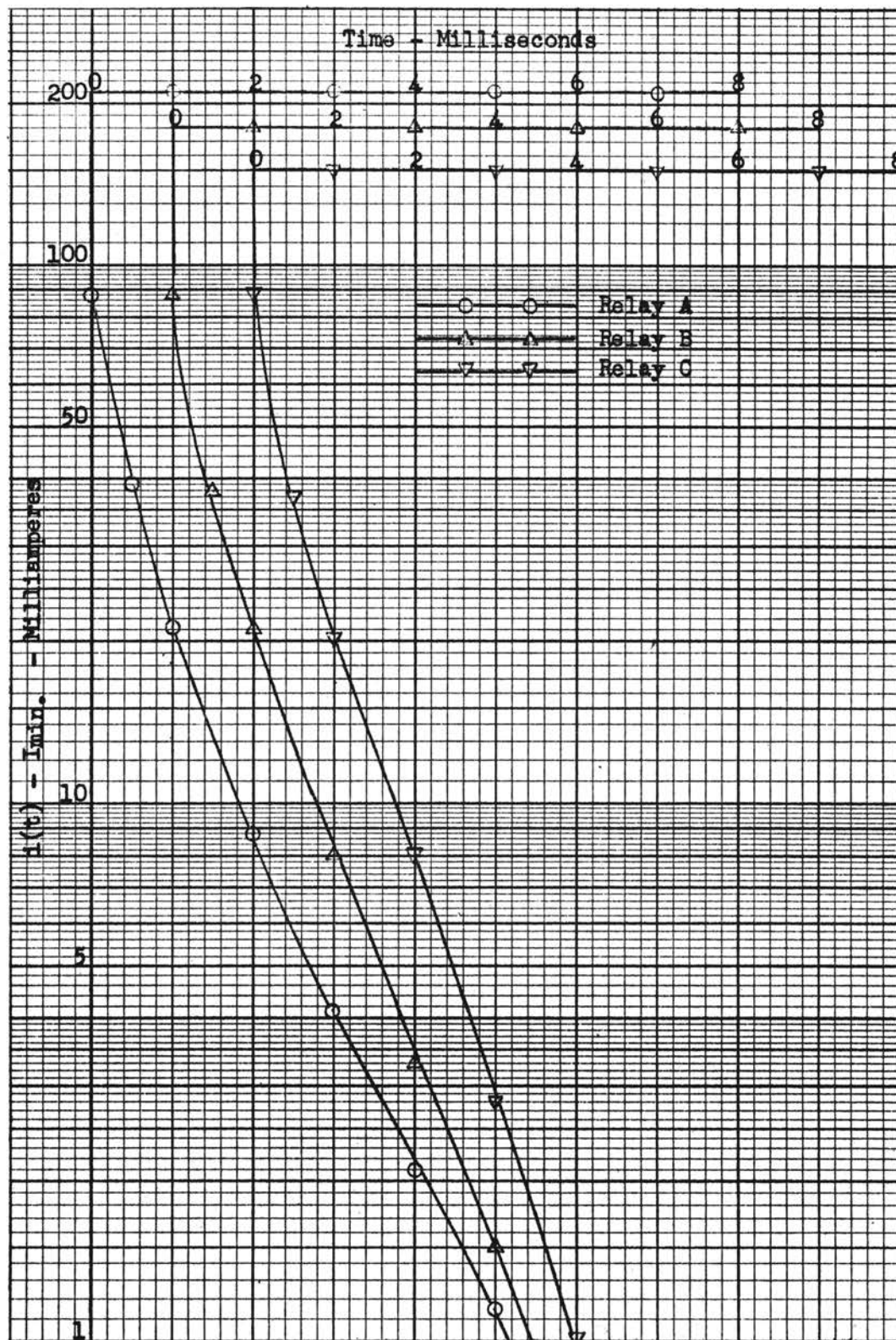


FIGURE 28 - RELAY COIL CURRENTS WITH STEP DECREASE FROM 28 TO 7 VOLTS D-C

CHAPTER V

CONCLUSIONS AND RECOMMENDATIONS

A word of caution is in order at this point before proceeding with the conclusions of this study. Since the scope of this study has been limited to relays of one particular type, extreme care should be exercised in applying these conclusions to relays in general. No assumption should be made concerning the general application of any conclusion unless it is specifically stated herein.

Reference to Table XV indicates that Method 2 is a method of energy calculation with sufficient accuracy for practical applications. The observed accuracy of Method 2 is especially good for Conditions 1 and 2 which are normal relay conditions. It is believed that this method will warrant general application since the effect of varying inductance is offset by the concept of calculating inductive energy for each small time increment. Condition 1 measurements appear to be more accurate than Condition 2, but Condition 2 accuracy may be improved by using a smaller discharge resistance to lengthen the discharge period. Method 3 does not show a consistent pattern of accuracy. Method 4 shows promise of reasonable accuracy and needs further investigation.

Reference to Table XVII indicates that the inductance of MHJ-18D relays is fairly consistent between specimens and will usually vary within plus or minus 10% of the mean.

It is recommended that Method 2 be used for measurements of

inductive energy on hermetically sealed relays. The degree of accuracy observed for the energy measurements on the one specimen and the consistency of inductance values of the three relays suggest that the inductive energy input calculated by Method 2 will be reasonably accurate for any Allied MHJ-18D relay at this operating voltage. However, safety factors should be applied for the observed errors plus the expected variation in relay coil resistance and the unknown errors in measurements and data processing. A safety factor of 100% is recommended until further investigation or experience provides better confidence in the observed data. The 100% safety factor is also recommended when applying Method 2 to other types of relays.

Method 3 is not recommended for practical application. Method 4 should be used sparingly, and only for preliminary estimates, until further investigation is made.

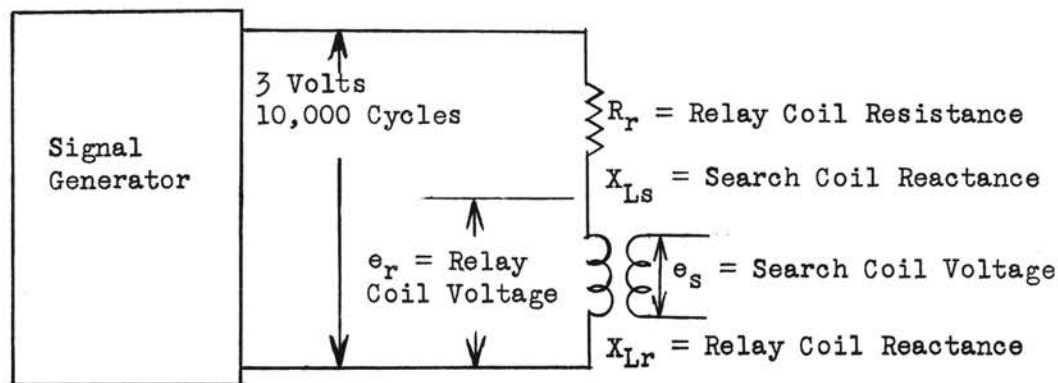
It is recommended that studies of the type made during this investigation, both energy and inductance, be performed on relays of other manufacturers, types, and ratings.

BIBLIOGRAPHY

1. Delalio, Louis D. and Charles P. Nunn. The D-C Inductive Loading of Contacts. A paper presented at the Eighth National Conference on Electro-Magnetic Relays, Oklahoma State University.
2. Mueller, George V. Introduction to Electrical Engineering (2nd. ed., New York, 1948).
3. Rudenberg, Reinhold V. Transient Performance of Electrical Power Systems (1st. ed., New York, 1951).
4. Cameron, C. F. and D. D. Lingelbach. Transient Coil Current as a Means of Relay Evaluation.
5. Peak, R. L., Jr. and H. N. Wagar. Switching Relay Design (Princeton, 1955).
6. Kelly, M. J. and J. E. Wallace. "The Analytical Design and Evaluation of Electromagnetics." Communications and Electronics, A I E E, 1957.

APPENDIX A

DETERMINATION OF COUPLING COEFFICIENTS



$$R_r = 210 \text{ ohms}$$

$$X_{Lr} \cong 60,000 \text{ ohms at } 10,000 \text{ cycles}$$

$$N_r = 4450 \text{ turns, } N_s = 72 \text{ turns}$$

The 3 volt, 10,000 cycle signal was applied to the input of the relay coil. Since $X_{Lr} \gg R_r$, the voltage drop across R_r is negligible.

The following values of e_s were measured with the vacuum tube voltmeter:

$$\text{With armature open, } e_s = 24 \text{ millivolts}$$

$$\text{With armature closed, } e_s = 34 \text{ millivolts}$$

The coefficient of coupling, K_c , is equal to the turn ratio divided by the voltage ratio. Turns ratio = $\frac{4450}{72} = 61.8$.

With armature open:

$$\text{Voltage ratio} = \frac{3}{.024} = 125.0$$

$$K_c = \frac{61.8}{125} = 0.495$$

With armature closed:

$$\text{Voltage ratio} = \frac{3}{.034} = 88.24$$

$$K_c = \frac{61.8}{88.24} = 0.7$$

APPENDIX B

DERIVATION OF FORMULA TO CALCULATE L FROM SEMI-LOG

PLOT OF LN i(t) VS t

For decaying exponential function:

$$i(t) = I_{\max} e^{-\frac{Rt}{L}}$$

$$\ln i(t) = \ln I_{\max} - \frac{R}{L} t$$

$$\frac{R}{L} t = \ln I_{\max} - \ln i(t)$$

$$\frac{R}{L} = \frac{\ln I_{\max} - \ln i(t)}{t}$$

= Slope of curve

where i(t) = instantaneous
current in amperes
I_{max} = steady state
current in amperes
L = circuit inductance
in henries
R = circuit resistance
in ohms

For small increments of time (Δt), the initial current (i₁) and final current (i₂) may be substituted in the slope formula for I_{max} and i(t), respectively.

$$\text{Slope} = \frac{\ln i_1 - \ln i_2}{\Delta t} = \frac{R}{L}$$

$$L = \frac{R}{\text{Slope}}$$

For increasing exponential function:

$$i(t) = I_{\max} \left(1 - e^{-\frac{Rt}{L}} \right)$$

$$= I_{\max} - I_{\max} e^{-\frac{Rt}{L}}$$

$$\frac{R}{L} t = \ln I_{\max} - \ln [I_{\max} - i(t)]$$

The above expression shows that I_{max} - i(t) may be plotted in lieu of i(t) for an increasing function.

$$\begin{aligned}\text{Slope} &= \frac{\ln i_1 - \ln i_2}{\Delta t} \\ &= \frac{R}{L}\end{aligned}$$

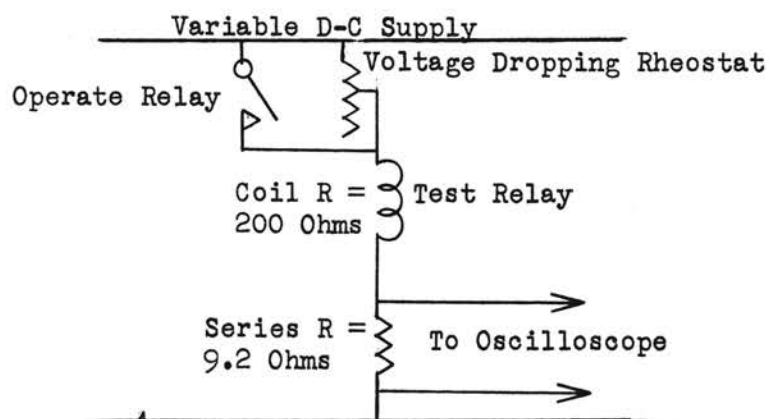
$$L = \frac{R}{\text{Slope}}$$

where i_1 and i_2 are initial and final values, respectively, during Δt from the plot of $I_{\max} - i(t)$ vs t .

APPENDIX C

METHOD FOR DROPPING VOLTAGE USED IN PROCEDURES

7 AND PROCEDURE 9 THROUGH 12



Only the relay coil circuit is shown in the above diagram. Otherwise the test circuit is the same as Figure 6. No discharge resistor was used for the test relay.

The values of voltage dropping resistance for the various procedures are as follows:

Procedure 7 - 570 ohms

Procedures 9 and 11 - 130 ohms

Procedure 10 - 290 ohms

Procedure 12 - 610 ohms

VITA

Robert Austin Cromwell

Candidate for the Degree of
Master of Science

Thesis: INVESTIGATION OF INDUCTIVE ENERGY RELATIONSHIPS IN RELAY
MAGNETIC CIRCUITS

Major Field: Electrical Engineering

Biographical:

Personal Data: Born at Buena Vista, Arkansas, March 13, 1922,
the son of Martin A. and Nina Cromwell.

Education: Attended grade school in Buena Vista, Arkansas;
graduated from Buena Vista High School in 1939; attended
the University of Arkansas; received the Bachelor of
Science degree from Texas Agricultural and Mechanical
College, with a major in Electrical Engineering, in August,
1950; completed requirements for the Master of Science
degree in August, 1961.

Professional experience: Was employed by the Arkansas Power
and Light Company as a Distribution Engineer from 1950 to
1951 and as a Relay Engineer from 1951 to 1956; has been
employed by the Douglas Aircraft Company since 1956 in
electrical design and reliability engineering; is a
Registered Professional Engineer in the State of Arkansas.